

## RESULTS AND DISCUSSION

### **1. Comparing NMR calculations of nevirapine in gas phase and solvation models**

Calculated  $^1\text{H}$ -NMR chemical shifts at B3LYP/6-311++G\*\*//B3LYP/6-31G\*\* level in gas and different IEF-PCM solvent models show different data. It is shown in Table 2 that IEF-PCM affects to the chemical shifts calculations. The chemical shifts of H23 proton in gas, DMSO, chloroform and dichloromethane are similar in the range of 6.17-6.52 ppm, but it is about 2 ppm less for the shifts in ethanol, methanol and water calculations. Considering to chemical shifts of H24 proton which is close to oxygen atom of 7-membered ring, the chemical shifts in solvent models are very smaller than the one in gas phase. Chemical shifts of H28 in DMSO, ethanol, methanol and water are negative that means this proton is more shielded than protons of TMS and because H28 is a proton of methyl group attached to a pyridine ring, the chemical shift value of this proton should not be negative. The H27, H28 and H29 are methyl protons that should show similar shifts, but the results from in solvent calculations are very different. For DMSO, chloroform and dichloromethane which are non-polar solvents show similar chemical shifts but different to polar solvents, ethanol, methanol and water. It shows that NMR calculations with IEF-PCM using GAUSSIAN98 still cannot represent good results.

For  $^{13}\text{C}$ -NMR chemical shifts calculations, most of  $^{13}\text{C}$  chemical shifts give similar results for gas, DMSO, chloroform, dichloromethane, ethanol, methanol and water solvation models except C16 which is the carbon of methyl group attached to a pyridine ring as shown in Table 3. The chemical shifts obtained from solvent calculations are smaller than gas phase calculations and show negative values for DMSO, dichloromethane, ethanol, methanol and water. Similarly to the  $^1\text{H}$ -NMR chemical shifts, IEF-PCM solvation model does not give reasonable results to methyl group of nevirapine. Different to the calculated  $^{15}\text{N}$ -NMR chemical shifts as shown in Table 4, the shifts seem to be similar between gas and solvent phase calculations. That is because the range of chemical shifts of  $^{15}\text{N}$  is very large comparing to  $^1\text{H}$  and  $^{13}\text{C}$  shifts. The negative chemical shift values indicate that there is more shielding in the

specified molecule than the reference molecule, and positive number indicates that there is less shielding than in the reference molecule.

**Table 2** Calculated  $^1\text{H}$ -NMR chemical shifts (ppm) in different solvents

$^1\text{H}$ -NMR	Gas	DMSO	$\text{CHCl}_3$	$\text{CH}_2\text{Cl}_2$	EtOH	MeOH	$\text{H}_2\text{O}$
21 H	8.41	7.49	7.82	7.61	7.08	7.06	7.02
22 H	7.01	9.13	8.46	8.81	10.63	10.70	10.83
23 H	6.46	6.17	6.52	6.24	4.52	4.47	4.39
24 H	8.37	2.60	3.69	3.45	2.15	2.05	1.76
25 H	7.05	10.05	9.13	9.53	11.41	11.51	11.69
26 H	8.75	9.39	9.21	9.25	9.59	9.62	9.68
27 H	2.20	1.70	1.68	1.76	2.11	2.12	2.13
28 H	2.18	-0.19	0.91	0.17	-2.26	-2.35	-2.51
29 H	2.33	0.20	0.75	0.49	0.12	0.08	0.01
30 H	3.81	0.83	1.71	1.42	0.04	-0.08	-0.28
31 H	0.34	1.16	1.17	0.98	0.91	0.94	0.98
32 H	0.93	1.23	1.17	1.14	0.53	0.53	0.54
33 H	0.94	2.08	1.73	1.82	1.40	1.43	1.48
34 H	0.41	0.99	0.74	0.87	0.73	0.75	0.78

**Table 3** Calculated  $^{13}\text{C}$ -NMR chemical shifts (ppm) in different solvents

$^{13}\text{C}$ -NMR	Gas	DMSO	$\text{CHCl}_3$	$\text{CH}_2\text{Cl}_2$	EtOH	MeOH	$\text{H}_2\text{O}$
2 C	150.90	144.70	146.93	145.22	139.53	139.41	139.19
3 C	126.38	110.91	116.23	113.26	102.17	101.67	100.77
4 C	143.00	137.72	139.91	138.48	133.11	132.90	132.55
6 C	173.95	180.53	179.74	179.53	179.50	179.56	179.81
7 C	148.08	142.64	142.58	143.37	150.65	150.73	150.55
8 C	123.04	120.17	121.16	120.62	117.66	117.53	117.27
9 C	159.68	161.43	160.90	160.67	156.78	156.85	157.00
12 C	161.67	166.78	165.55	165.73	169.20	169.39	169.73
13 C	133.92	130.00	132.45	130.48	125.04	124.85	124.54
14 C	126.13	125.83	125.15	125.78	126.16	126.22	126.33
15 C	168.65	185.10	181.35	182.01	182.51	182.85	183.59
16 C	19.71	-7.33	0.87	-3.71	-16.81	-17.47	-18.64
17 C	35.45	34.73	35.12	34.85	37.12	37.15	37.19
18 C	13.36	21.48	19.43	19.68	15.49	15.67	16.01
19 C	12.89	18.21	17.09	16.99	12.90	13.01	13.18

**Table 4** Calculated  $^{15}\text{N}$ -NMR chemical shifts (ppm) in different solvents

$^{15}\text{N}$ -NMR	Gas	DMSO	$\text{CHCl}_3$	$\text{CH}_2\text{Cl}_2$	EtOH	MeOH	$\text{H}_2\text{O}$
1 N	-85.26	-83.67	-84.50	-85.09	-79.67	-79.22	-78.49
5 N	-265.94	-288.57	-275.35	-285.14	-322.65	-323.81	-325.79
10 N	-87.90	-85.57	-85.62	-85.82	-85.57	-85.29	-84.74
11 N	-268.54	-273.95	-271.27	-271.84	-273.95	-273.89	-273.83

## 2. Conformational analysis of nivirapine and NMR calculations

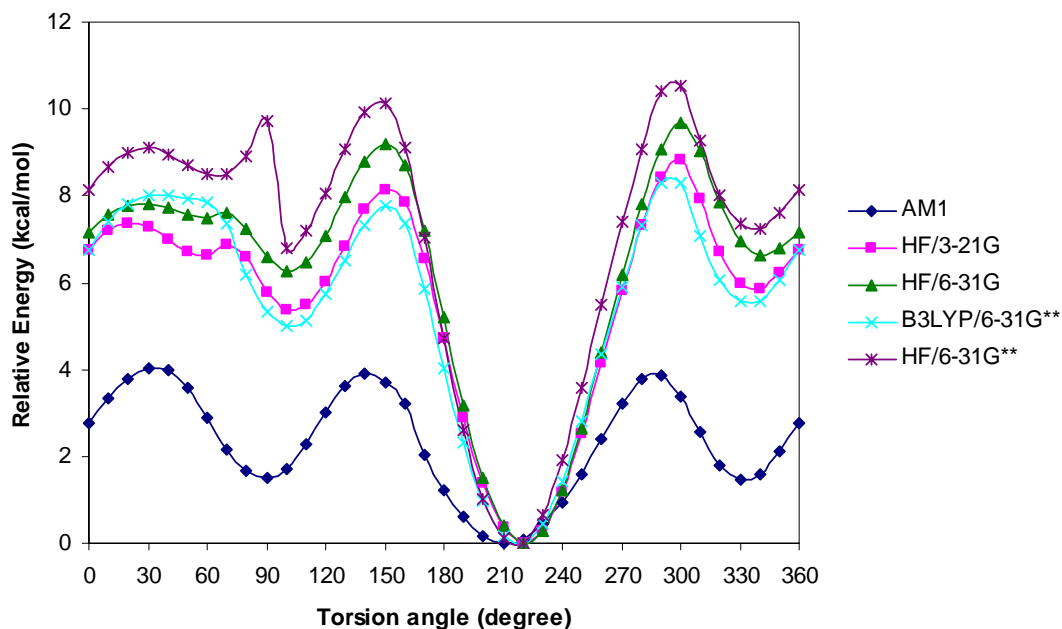


**Figure 4** Rotational potential (kcal/mol) of dihedral angle  $\alpha$  obtained from AM1, HF/3-21G level, HF/6-31G level, HF/6-31G\*\* level, and B3LYP/6-31G\*\* level of calculations.

The determination of conformational minima of nevirapine was studying by using GAUSSIAN03. The dihedral angles which determine the position of the cyclopropyl ring (C15-N11-C17-C19,  $\alpha$ ) were analyzed by using AM1, HF/3-21G, HF/6-31G, HF/6-31G\*\*, and B3LYP/6-31G\*\* methods as shown in Figure 4. From the results, it can be seen that *ab initio* and DFT methods of calculations lead to the same conformational minimum where the dihedral angle  $\alpha$  is equal to 220°. Moreover, at  $\alpha$  angles around 100° and 340°, two other energy minima can be observed, with not too high energy barriers between them (2-3 kcal/mol). Except the results from AM1 method, the three conformational minima are 10° different from *ab initio* and DFT methods,  $\alpha$  around 90°, 210° and 330°. It shows that AM1 which is a semiempirical method give a little bit different results for conformational analysis comparing to *ab initio* and DFT methods for this system.

The three conformational minima at  $\alpha = 100^\circ$ ,  $220^\circ$  and  $340^\circ$  from the conformation analysis were fully optimized at B3LYP/6-31G\*\* level. The obtained structural parameters with the lowest energy conformation calculated were compared with X-ray diffraction data of nevirapine complex with RT and presented in Table 5. The full optimizations of the starting geometries of each conformational minima of nevirapine show  $\alpha = 101.8^\circ$ ,  $217.4^\circ$  and  $334.3^\circ$ . The energy minimum at  $\alpha = 217.4^\circ$  ( $\alpha_{\text{Expt.}} = 208.5^\circ$ ) gives the smallest standard deviation (7.7) and it gives the same optimum structure of the full optimization at B3LYP/6-31G\*\* level. Superimposition of the geometry optimization at B3LYP/6-31G\*\* level on the crystal structure of nevirapine in the complex shows good agreement (root mean square deviation of 0.08). From these results, it can be seen that the dihedral angle  $\alpha$  is restricted to the one minimum at  $\alpha = 217.4^\circ$ . Considering the position of the energy minimum at  $\alpha = 217.4^\circ$  in more details and by comparing to the experimental values obtained by X-ray investigation, it shows that the calculated values are nearly the same as the experimental ones. This can be seen to suggest that the conformation of nevirapine in the inhibition complex is rather close to its energy minimum conformation.

**Table 5** Comparison of the selected torsion angles of the fully optimized geometries of nevirapine, obtained by each local minima at  $\alpha = 100$ ,  $\alpha = 220$  and  $\alpha = 340$  degrees and compared to experimental X-ray crystallographic data<sup>a</sup>

Torsion angle	Expt.	Starting geometry obtained from		
		$\alpha = 100$	$\alpha = 220$	$\alpha = 340$
		B3LYP/6-31G**		
		$\alpha = 101.8$	$\alpha = 217.4$	$\alpha = 334.3$
O20-C6-C14-C7	30.0	19.2	21.2	23.4
C12-N11-C17-C19	68.7	305.4	71.2	179.5
C12-N11-C17-C18	136.8	22.8	139.9	257.1
C14-C15-N11-C17	168.3	152.0	159.9	151.5
C13-C12-N11-C17	200.1	215.2	205.4	215.2
<b>C15-N11-C17-C19</b>	<b>208.5</b>	<b>101.8</b>	<b>217.4</b>	<b>334.3</b>
C15-N11-C17-C18	276.6	175.7	286.1	51.9
C6-N5-C13-C14	144.4	129.5	134.8	135.9
N5-C6-C14-C7	212.9	197.9	201.1	204.2
C15-N11-C12-N1	238.8	239.2	238.0	236.5
C12-N11-C15-N10	126.7	132.4	127.9	126.8
SD <sup>b</sup>		95.8	7.7	96.8

<sup>a</sup> Data obtained from resolution of 2.2 Å (Ren *et al.*, 1995)

<sup>b</sup> Standard deviation (SD) =  $[\sum(x_{\text{Cal.}} - x_{\text{Expt.}})^2 / n - 1]^{1/2}$

**Table 6** Comparison of experimental and calculated  $^1\text{H}$ -NMR chemical shifts (ppm) at different  $\alpha$  angle (degree) of the cyclopropyl ring (C15-N11-C17-C19) calculated at B3LYP/6-311++G\*\*//B3LYP/6-31G\*\* level with DMSO and chloroform IEF-PCM solvation models.

$^1\text{H}$ - NMR	Chemical shifts $\delta$ (ppm) in DMSO				Chemical shifts $\delta$ (ppm) in chloroform			
		$\alpha =$	$\alpha =$	$\alpha =$		$\alpha =$	$\alpha =$	$\alpha =$
	Expt.	101.8	217.4	334.3	Expt.	101.8	217.4	334.3
21 H	8.06	8.40	8.59	8.59	8.16	8.33	8.53	8.54
22 H	7.04	7.52	7.56	7.42	6.94	7.36	7.40	7.25
23 H	9.86	7.13	7.09	7.16	8.69	6.91	6.88	6.93
24 H	8.00	8.67	8.63	8.55	8.11	8.62	8.58	8.50
25 H	7.17	7.43	7.51	7.46	7.07	7.29	7.36	7.31
26 H	8.50	8.98	8.98	8.79	8.54	8.91	8.90	8.70
27 H	2.32	2.43	2.36	2.43	2.41	2.38	2.30	2.37
28 H	2.32	2.26	2.27	2.29	2.41	2.21	2.22	2.24
29 H	2.32	2.41	2.33	2.43	2.41	2.42	2.33	2.43
30 H	3.61	3.41	3.80	3.26	3.77	3.35	3.84	3.18
31 H	0.33	1.96	0.46	1.74	0.50	2.01	0.42	1.75
32 H	0.86	0.83	0.98	0.48	1.00	0.82	0.95	0.43
33 H	0.86	0.50	1.02	0.77	1.00	0.46	1.00	0.75
34 H	0.33	1.42	0.48	2.11	0.50	1.41	0.46	2.16
SD <sup>a</sup>		0.65	0.34	0.73		0.60	0.27	0.68

<sup>a</sup> Standard deviation (SD) =  $[\sum(x_{\text{Cal.}} - x_{\text{Expt.}})^2 / n - 1]^{1/2}$ , excluded H23

**Table 7** Comparison of experimental and calculated  $^{13}\text{C}$ -NMR chemical shifts (ppm) at different  $\alpha$  angle (degree) of the cyclopropyl ring (C15-N11-C17-C19) calculated at B3LYP/6-311++G\*\*//B3LYP/6-31G\*\* level with DMSO and chloroform IEF-PCM solvation models.

$^{13}\text{C}$ - NMR	Chemical shifts $\delta$ (ppm) in DMSO				Chemical shifts $\delta$ (ppm) in chloroform			
		$\alpha =$	$\alpha =$	$\alpha =$		$\alpha =$	$\alpha =$	$\alpha =$
	Expt.	101.8	217.4	334.3	Expt.	101.8	217.4	334.3
2 C	140.73	151.77	152.22	153.62	140.36	151.26	151.87	153.23
3 C	120.91	129.29	128.80	129.06	120.22	128.55	128.04	128.30
4 C	140.01	148.05	146.99	146.87	139.47	146.93	145.71	145.58
6 C	167.02	178.08	176.74	177.11	168.85	177.25	175.96	176.28
7 C	143.59	149.99	149.39	149.37	144.31	149.63	148.99	149.07
8 C	119.35	124.03	124.88	124.92	118.97	123.41	124.21	124.28
9 C	151.33	161.73	161.83	160.88	152.1	161.11	161.22	160.16
12 C	154.20	159.12	162.27	162.41	153.95	159.15	162.24	162.34
13 C	124.92	135.69	135.13	134.67	124.9	135.47	134.76	134.31
14 C	122.27	125.81	126.81	128.18	122.08	125.54	126.53	128.02
15 C	159.99	170.54	169.83	167.91	160.55	170.23	169.58	167.71
16 C	17.57	19.80	19.73	20.02	17.80	19.78	19.70	19.99
17 C	29.29	42.65	35.64	43.27	29.61	42.72	35.59	43.40
18 C	8.52	1.47	13.24	8.97	8.82	1.50	13.26	9.07
19 C	8.75	9.75	12.57	0.80	9.11	9.83	12.60	0.90
SD <sup>a</sup>		8.65	7.93	8.71		8.10	6.43	8.22

$$^a \text{Standard deviation (SD)} = [\sum(x_{\text{Cal.}} - x_{\text{Expt.}})^2 / n - 1]^{1/2}$$

To test the correlation between the conformational analysis results with structures in solution, the NMR shifts in of nevirapine in solutions were calculated. The chemical shifts of three conformational minima were calculated using DMSO and chloroform solvation models and then compared to experimental results. Comparing between our experimental data to the previously reported experimental  $^1\text{H}$  NMR chemical shifts for nevirapine in DMSO-*d*6 (Hargrave *et al.*, 1991) and  $^{13}\text{C}$ -NMR chemical shifts in  $\text{CDCl}_3$  (Norman *et al.*, 1993), showed standard deviations of about 0.01 and 0.02 for the  $^1\text{H}$  and  $^{13}\text{C}$ -NMR chemical shifts, respectively. The results for  $^1\text{H}$ ,  $^{13}\text{C}$ -NMR chemical shifts are shown in Table 6 and 7.

As expected, it was found that the optimum geometry at  $\alpha = 217.4^\circ$  shows an good agreement between calculated  $^1\text{H}$  chemical shifts and experimental data, except the  $^1\text{H}$  chemical shift of the H23 atom attached to the nitrogen atom of the 7 membered ring. Because this proton is an acidic proton, hydrogen bonding strongly influences the electronic environment of this proton in solution. Studying in more details about H23 chemical shifts will be presented in MD section. The H27, H28, H29 and C16 atoms of methyl group which did not show a good agreement to the experiment results in solvent calculations of GAUSSIAN98, give very good data for this study.

Considering the H30, H31, H34, H32 and H33 calculated chemical shifts which are influenced by the rotation around the alpha angle, these shifts are completely different at  $\alpha = 101.8^\circ$  and  $\alpha = 334.3^\circ$ , but similar at  $\alpha = 217.4^\circ$ , to the experimental data. The same with the 17C, 18C and 19C calculated chemical shifts in that they are similar to the experimental data only at  $\alpha = 217.4^\circ$ . It can be seen that the chemical shifts of cyclopropyl ring are very sensitive to the rotation around the alpha angle. Plots of the  $^1\text{H}$ - and  $^{13}\text{C}$ -NMR chemical shifts in DMSO and chloroform as calculated against experimental data are shown in Figure 5. With  $\alpha = 217.4^\circ$ , correlation coefficients are  $R^2 = 0.991$  for  $^1\text{H}$ -NMR in chloroform, and  $R^2 = 0.999$  for  $^1\text{H}$ -NMR in DMSO and  $^{13}\text{C}$ -NMR in both solvents. This shows good agreement and the presence of a conformation of nevirapine in DMSO and chloroform solutions consistent with the optimized geometry at a dihedral angle  $\alpha$  of about  $217.4^\circ$ .

To investigate in more detail, the plots between calculated and experimental chemical shifts of protons and carbons located in the cyclopropyl ring H30 H31, H32, H33, H34, C17, C18 and C19 at different alpha angles in DMSO and chloroform were considered. From the plots in Figure 6, it is obviously seen that the rotation around alpha angle effects the shifts of atoms in the cyclopropyl ring and it shows the best agreement between calculated and experimental chemical shifts at  $\alpha = 217.4^\circ$ .

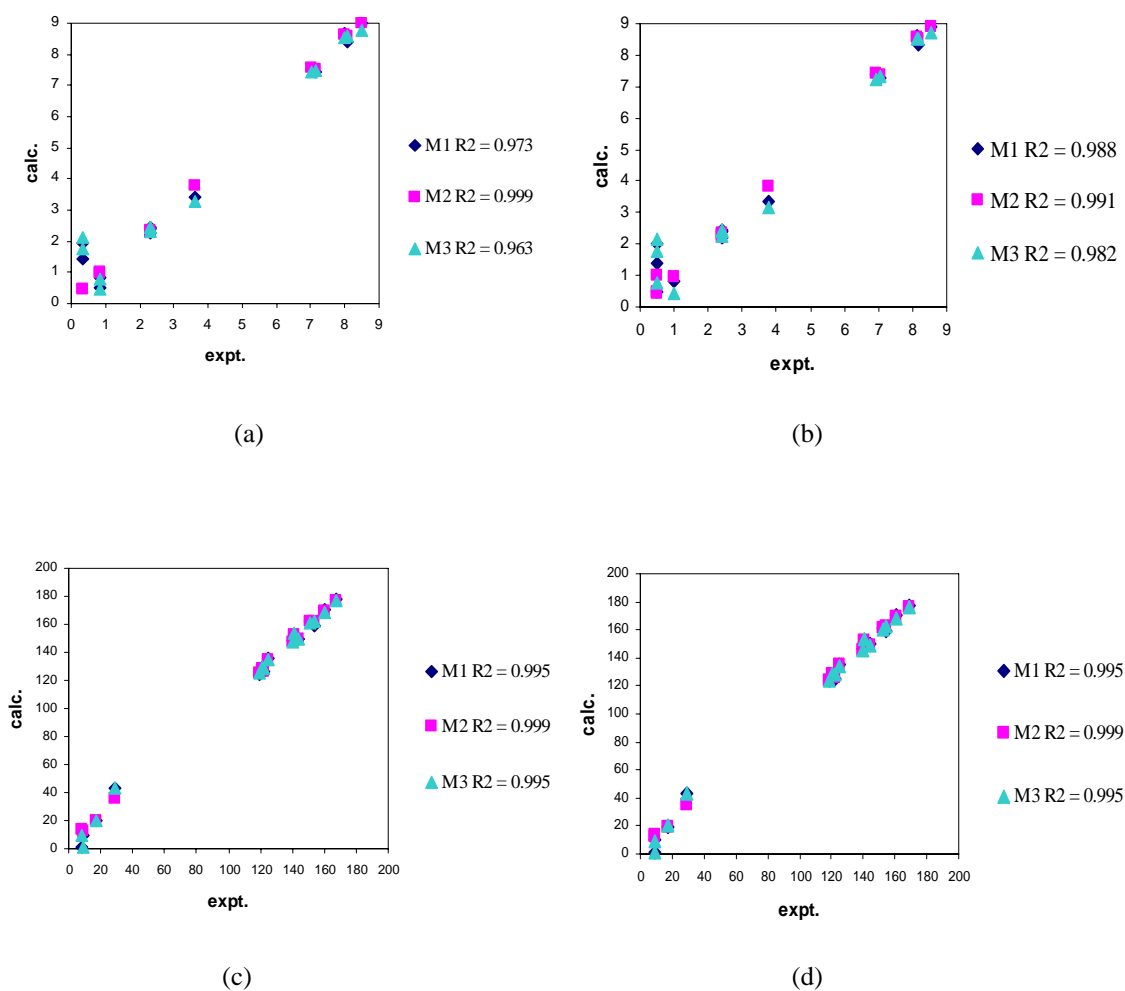


**Figure 5** Correlation plots between calculated and experimental chemical shifts (ppm) for the  $\alpha = 101.8$  (M1),  $\alpha = 217.4$  (M2) and  $\alpha = 334.3$  (M3) (a)  $^1\text{H-NMR}$  chemical shifts in DMSO, (b)  $^1\text{H-NMR}$  chemical shifts in chloroform, (c)  $^{13}\text{C-NMR}$  chemical shifts in DMSO and (d)  $^{13}\text{C-NMR}$  chemical shifts in chloroform.

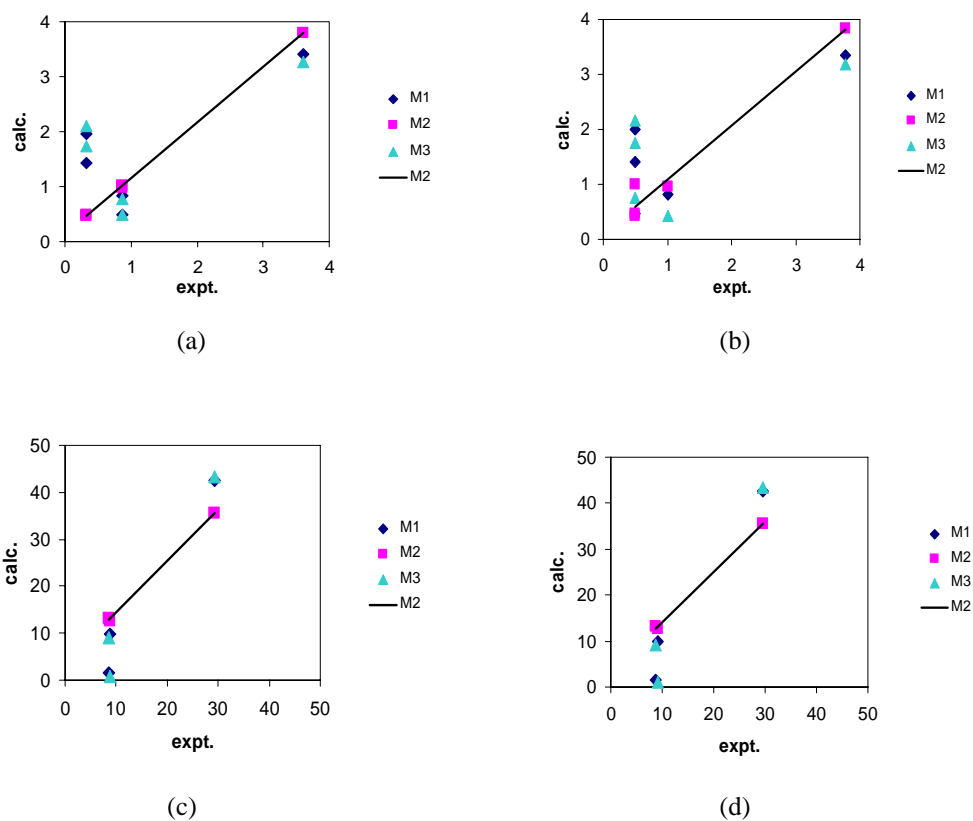


**Figure 6** Correlation plots between calculated and experimental chemical shifts (ppm) of H30, H31, H32, H33, H34, C17, C18 and C19 for the  $\alpha = 101.8$  (M1),  $\alpha = 217.4$  (M2) and  $\alpha = 334.3$  (M3) (a)  $^1\text{H-NMR}$  chemical shifts in DMSO, (b)  $^1\text{H-NMR}$  chemical shifts in chloroform, (c)  $^{13}\text{C-NMR}$  chemical shifts in DMSO and (d)  $^{13}\text{C-NMR}$  chemical shifts in chloroform.

**Table 8** Comparison of experimental and calculated  $^{15}\text{N}$ -NMR chemical shifts (ppm) at different  $\alpha$  angle (degree) of the cyclopropyl ring (C15-N11-C17-C19) calculated at B3LYP/6-311++G\*\*//B3LYP/6-31G\*\* level with DMSO IEF-PCM solvation models.

$^{15}\text{N}$ - NMR	Chemical shifts $\delta$ (ppm) in DMSO						
	Expt.	$\alpha = 101.8$	residual	$\alpha = 217.4$	residual	$\alpha = 334.3$	residual
1 N	-91.6	-99.7	8.1	-108.5	16.9	-105.2	13.6
5 N	-252.3	-270.5	18.2	-272.7	20.4	-272.3	20.0
10 N	-89.6	-105.2	15.6	-107.6	18.0	-104.3	14.7
11 N	-269.4	-291.6	22.2	-280.8	<b>11.4</b>	-297.4	28.0

As  $^{15}\text{N}$ -NMR chemical shifts are very sensitive to environmental changes, considering the  $^{15}\text{N}$ -NMR chemical shifts of nevirapine at all three conformational angles was of great interest. The prediction of the  $^{15}\text{N}$ -NMR chemical shifts is shown in Table 8 and 9. The results indicate that N1, N10 and N11 were affected by the rotational angle. This is especially so for N11, which forms the single bond to carbon (N11-C17) which rotates, and shows completely different chemical shifts at the three different alpha angles. The ranges of N11 chemical shifts are -280.8 to -297.4 ppm in DMSO and -277.5 to -294.4 ppm in chloroform solutions respectively. Unlike N5 which, being distant from the cyclopropyl ring, has chemical shifts that do not seem to be much affected. Residual between calculated and experimental shifts of N11 at  $\alpha = 217.4^\circ$  is smallest (11.4 ppm) comparing to  $\alpha = 101.8^\circ$  and  $\alpha = 334.3^\circ$  in both DMSO and chloroform.

The correlation coefficients of all three conformational angles in both solvents are similar about 0.99 as shown in Figure 7.

**Table 9** Comparison of experimental and calculated  $^{15}\text{N}$ -NMR chemical shifts (ppm) at different  $\alpha$  angle (degree) of the cyclopropyl ring (C15-N11-C17-C19) calculated at B3LYP/6-311++G\*\*//B3LYP/6-31G\*\* level with chloroform IEF-PCM solvation models.

$^{15}\text{N}$ - NMR	Chemical shifts $\delta$ (ppm) in chloroform						
	Expt.	$\alpha = 101.8$	residual	$\alpha = 217.4$	residual	$\alpha = 334.3$	residual
1 N	-91.1	-100.9	9.8	-101.7	10.6	-98.8	7.7
5 N	-248.6	-274.7	26.1	-271.0	22.4	-270.7	22.1
10 N	-86.3	-105.8	19.5	-101.8	15.5	-100.1	13.8
11 N	-264.4	-294.4	30.0	-277.5	<b>13.1</b>	-294.1	29.7

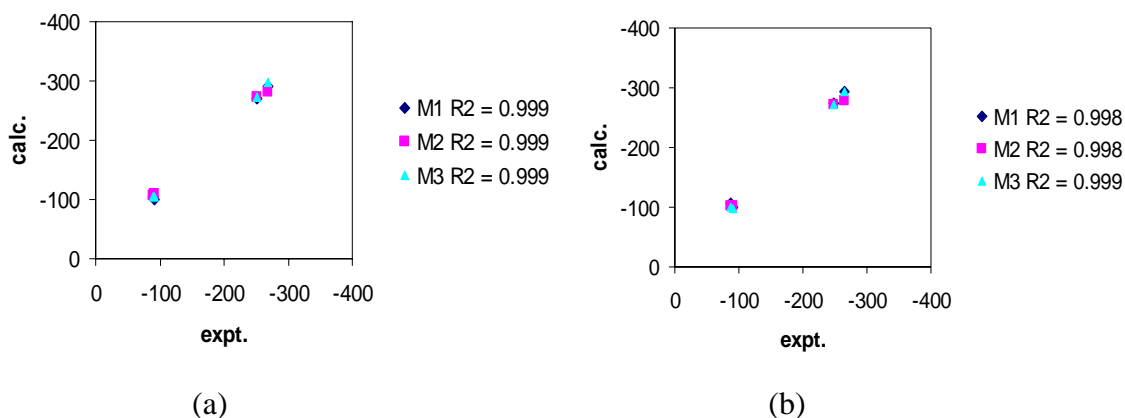


**Figure 7** Correlation plots between calculated and experimental chemical shifts (ppm) of N1, N5, N10, and N11, for the  $\alpha = 101.8$  (M1),  $\alpha = 217.4$  (M2) and  $\alpha = 334.3$  (M3) (a)  $^{15}\text{N}$ -NMR chemical shifts in DMSO, (b)  $^{15}\text{H}$ -NMR chemical shifts in chloroform

**Table 10** Calculated energies of nevirapine at B3LYP/6-311++G\*\*// B3LYP/6-31G\*\* level in the gas phase and solution<sup>a</sup>.

Nevirapine	$\Delta E^{\text{gas phase}}$	$\Delta E^{\text{iefpcm}}$	$\Delta G_{\text{sol}}^{\text{b}}$	$\Delta G_{\text{elec}}$	$\Delta G_{\text{cav}}$	$\Delta G_{\text{dis}}$	$\Delta G_{\text{rep}}$
DMSO, $\epsilon = 46.7$							
$\alpha = 101.8^\circ$	5.53	6.13	-1.18	-11.44	32.92	-24.12	1.46
$\alpha = 217.4^\circ$	0	0	-1.77	-12.25	33.07	-24.07	1.49
$\alpha = 334.3^\circ$	6.03	6.21	-1.59	-11.85	32.94	-24.14	1.46
CDCl <sub>3</sub> , $\epsilon = 4.9$							
$\alpha = 101.8^\circ$	5.53	5.85	-0.13	-8.07	24.77	-17.79	0.95
$\alpha = 217.4^\circ$	0	0	-0.44	-8.55	24.88	-17.74	0.97
$\alpha = 334.3^\circ$	6.03	6.11	-0.37	-8.31	24.79	-17.80	0.95

<sup>a</sup> Energies (E) and all free energies changes ( $\Delta G$ ) are in kcal/mol

<sup>b</sup>  $\Delta G_{\text{sol}} = \Delta G_{\text{elec}} + \Delta G_{\text{cav}} + \Delta G_{\text{dis}} + \Delta G_{\text{rep}}$

The calculated free energy changes of solvation of nevirapine at all three alpha conformations are shown in Table 10. The solvation free energy ( $\Delta G_{\text{sol}}$ ) is defined as the free energy change to transfer a molecule from vacuum to solvent. The  $\Delta G_{\text{sol}}$  can be considered to have three components:  $\Delta G_{\text{elec}}$ ,  $\Delta G_{\text{cav}}$ , and  $\Delta G_{\text{dis}}$  and  $\Delta G_{\text{rep}}$ ; where  $\Delta G_{\text{elec}}$  stands for the electrostatic component,  $\Delta G_{\text{cav}}$  presents the free energy required to form the solute cavity within the solvent,  $\Delta G_{\text{dis}}$  and  $\Delta G_{\text{rep}}$  are the dispersion and repulsion contribution (van der Waals interaction between the solute and the solvent). It is shown that the different alpha conformational angles present different energies in gas phase and in solution models. The range of  $\Delta E$  of nevirapine in gas phase is between 5.53-6.03 kcal/mol and the range of  $\Delta E$  of nevirapine in DMSO and chloroform IEF-PCM models are 6.13-6.21 and 5.85-6.11 kcal/mol respectively. As expected, different alpha angles show different  $\Delta G_{\text{sol}}$  values. It can be concluded that the rotational alpha angle influences the solvation energies of nevirapine in DMSO and chloroform.

**Table 11** Experimental  $^{15}\text{N}$  chemical shifts<sup>a,b</sup>,  $\delta_{\text{expt}}$ , and calculated isotropic nitrogen shielding constants,  $\sigma_{\text{calc}}$  (ppm), calculated at B3LYP/6-311++G\*\*//B3LYP/6-31G\*\* level

		$\delta_{\text{expt}}$			$\sigma_{\text{calc}}$	
		DMSO	$\text{CDCl}_3$	Gas <sup>c</sup>	DMSO	$\text{CHCl}_3$
$\text{NH}_3$	N			258.7	262.6	261.4
Pyrolidine	N	37.3	37.9	192.4	194.8	192.9
N-methyl pyrrolidine	N	42.1	43.3	190	190.6	190.3
Piperdine	N	36.9	38.2	193.9	199.3	198.1
N-methyl piperidine	N	38.7	40.1	194.6	213.9	213.6
Aniline	N	59.0	54.4	185.5	190.3	190.9
N-methylaniline	N	53.0	51.5	182	186.4	187.3
N,N-dimethylaniline	N	44.8	43.9	189.6	189.2	190.5
Pyrrole	N	155.1	146.2	91.1	82.6	85.6
N-methyl pyrrole	N	150.0	148.8	83.4	77.4	79.4
Pyrazole	N-1	207.2	246.2	37.7	31.2	75.9
	N-2	299.9	246.2	-82.3	-63.9	-27.3
N-methyl pyrazole	N-1	202.2	199.9	28.0	25.3	26.1
	N-2	308.3	304.9	-91.3	-74.5	-79.5
Imidazole	N-1	211.2	207.8	85	71.8	75.9
	N-3	211.2	207.8	-43.5	-20.2	-27.2
N-methyl imidazole	N-1	161.5	159.3	73.6	64.4	67.3
	N-3	261.6	256.5	-43.9	-19.9	-26.5
Pyridine	N	316.7	311.6	-102.8	-80.1	-86.6
2-Picoline	N	315.7	310.1	-99.2	-80.3	-85.9
3-Picoline	N	311.6	305.9	-101.8	-78.7	-85.0
4-Picoline	N	303.4	297.6	-92.2	-70.8	-77.1
2,6-Lutidine	N	315.3	309.5	-97	-82.3	-82.3
Pyridazine	N	400.0	397.9	-217.9	-180.6	-191.3
Pyrimidine	N	295.3	293.3	-76.6	-61.0	-65.3
Pyrazine	N	333.8	331.5	-119.3	-104.6	-108.7
Indole	N	134.0	124.1	112.2	105.0	107.5
Quinoline	N	313.0	308.0	-98.5	-77.0	-83.4
Isoquinoline	N	310.8	305.4	-94	-72.5	-78.7
Phthalazine	N	369.4	365.9	-179.7	-142.8	-153.6
Quinazoline	N-1	283.1	280.8	-61.7	-48.8	-52.8
	N-3	294.4	291.3	-74.1	-56.8	-61.8
Quinoxaline	N	329.9	328.2	-114.5	-101.3	-105.1
Acridine	N	306.0	300.6	-90.5	-68.7	-75.8
Phenazine	N	326.4	323.3	-109.6	-96.7	-100.5

<sup>a</sup> Relative to external  $\text{NH}_3$

<sup>b,c</sup> (Dokalik et al., 1999)

**Table 12** Linear regressions between experimental chemical shifts<sup>a</sup> and calculated isotropic shielding constants (ppm),  $\delta_{\text{expt}} = a + b\sigma_{\text{calc}}$ , of nitrogen ( $R^2$  = correlation coefficient,  $SD^b$  = standard deviation)

	Parameter	B3LYP/6-311++G**//B3LYP/6-31G**		
		Gas <sup>c</sup>	DMSO	CHCl <sub>3</sub>
Nitrogen (DMSO)	a	224.0	235.2	-
	b	-0.9038	-0.9719	-
	R <sup>2</sup>	0.994	0.996	-
	SD	9.5	7.4	-
Nitrogen (CDCl <sub>3</sub> )	a	220.0	-	228.0
	b	-0.896	-	-0.9386
	R <sup>2</sup>	0.995	-	0.996
	SD	8.2	-	7.3

<sup>a</sup> Relative to external NH<sub>3</sub>

<sup>b</sup> Standard deviation (SD) =  $[\sum(x_{\text{Cal.}} - x_{\text{Expt.}})^2 / n - 1]^{1/2}$

<sup>a, c</sup> (Dokalik et al., 1999)

**Table 13** Predicted  $^{15}\text{N}$ -NMR chemical shifts,  $\delta$  (ppm), by B3LYP/6-311++G\*\*//B3LYP/6-31G\*\* calculations in DMSO and chloroform of nevirapine by using scaling theoretical data linear regressions,  $\delta_{\text{expt}} = a + b\sigma_{\text{calc}}$

$^{15}\text{N}$ -NMR	$\delta$ (ppm) in DMSO	$\delta$ (ppm) in chloroform
1 N	292.6	288.2
5 N	133.1	129.2
10 N	293.5	288.1
11 N	125.2	123.2

Following the approach of Dokalik and coworkers (Dokalik et al., 1999), the known  $^{15}\text{N}$ -NMR chemical shifts of a series of nitrogen-containing heterocycles can be used to make correlations between experimentally determined chemical shifts and GIAO-calculated isotropic shielding constants and predict the  $^{15}\text{N}$ -NMR chemical shifts. Experimental  $^{15}\text{N}$ -NMR chemical shifts, as obtained from  $\text{CDCl}_3$  and  $\text{DMSO-}d_6$  solutions and theoretical isotropic nitrogen shielding constants are given in Table 11. Nitrogen chemical shifts are known to be subject to appreciable solvent effects. It shows that the  $^{15}\text{N}$  shifts obtained from  $\text{DMSO-}d_6$  solution are on average shifted down-field by about 3.5 ppm relative to those from  $\text{CDCl}_3$  solutions, with a maximum difference of about 10 ppm. The plots between experimental  $^{15}\text{N}$  chemical shifts and calculated isotropic nitrogen shielding constants in DMSO and chloroform are shown in Figure 8. The linear regressions between experimental chemical shifts and calculated isotropic shielding constants (ppm),  $\delta_{\text{expt}} = a + b\sigma_{\text{calc}}$ , of nitrogens in DMSO and chloroform were made and the details are shown in Table 12. The SD values of predicted  $^{15}\text{N}$ -NMR chemical shifts in DMSO (SD = 7.3) and chloroform (SD = 7.4) models show better agreement comparing to the  $^{15}\text{N}$ -NMR chemical shifts

in gas phase (SD =9.5 and 8.2 respectively) which were performed with the GAUSSIAN94 program package by Dokalik and coworkers. It can be concluded that the IEF-PCM model improves the results of  $^{15}\text{N}$ -NMR chemical shifts in this case.

As the linear regressions of correlations between experimentally determined  $^{15}\text{N}$ -NMR chemical shifts and GIAO-calculated isotropic shielding constants in DMSO and chloroform IEF-PCM models are  $\delta_{\text{expt}} = 235.2 - 0.9719\sigma_{\text{calc}}$  and  $\delta_{\text{expt}} = 228.0 - 0.9386\sigma_{\text{calc}}$  respectively, the  $^{15}\text{N}$ -NMR chemical shifts of 4 nitrogen atoms in nevirapine molecule can be calculated. The calculated data relative to external  $\text{NH}_3$  are shown in Table 13. The positive numbers of all the chemical shifts indicate that all the nitrogen molecules of nevirapine are more de-shielding than the nitrogen of ammonia.

Because Marek and coworkers (Marek *et al.*, 2002) reported the interrelation of the  $^{15}\text{N}$ -NMR chemical shifts of  $\text{NH}_3$  and nitromethane is 379.8 ppm, the obtained  $^{15}\text{N}$ -NMR chemical shifts can be presented referring to nitromethane and compared to experimental results as shown in Table 14. The residuals of both calculations in DMSO and chloroform are small except of N11 atom which is a sensitive atom that forms single bond to carbon (N11-C17) and can rotate.

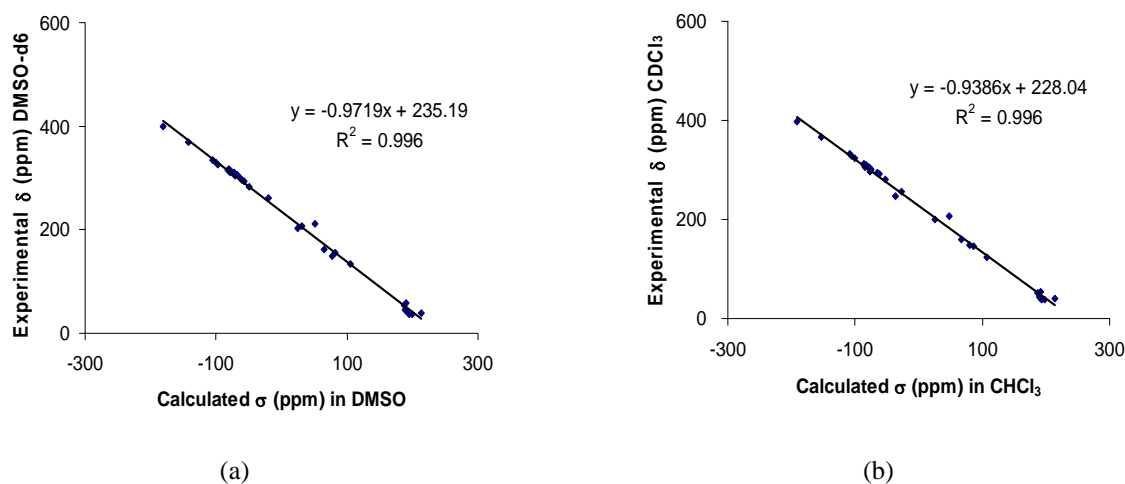


**Figure 8** Experimental  $^{15}\text{N}$ -NMR chemical shifts,  $\delta$ , versus calculated isotropic nitrogen shielding constants,  $\sigma$ , performed at B3LYP/6-311++G\*\*//B3LYP/6-31G\*\* level (a) DMSO (b) chloroform

**Table 14** Predicted  $^{15}\text{N}$ -NMR chemical shifts,  $\delta$  (ppm), by B3LYP/6-311++G\*\*//B3LYP/6-31G\*\* calculations in DMSO and chloroform of nevirapine by using scaling theoretical data linear regressions,  $\delta_{\text{expt}} = a + b\sigma_{\text{calc}}$

$^{15}\text{N}$ -NMR	Chemical shifts $\delta$ (ppm) in DMSO			Chemical shifts $\delta$ (ppm) in Chloroform		
	Expt.	Calc.	residual	Expt.	Calc.	residual
1 N	-91.6	-87.2	-4.4	-91.1	-91.6	0.5
5 N	-252.3	-246.7	-5.6	-248.6	-250.6	2.0
10 N	-89.6	-86.3	-3.3	-86.3	-91.7	5.4
11 N	-269.4	-254.6	-14.8	-264.4	-256.6	-7.8

### **3. Comparing of IEF-PCM solvation models and solvent optimization effects**

As PCM in GAUSSIAN03 program was improved from of GAUSSIAN98 program, it is interesting to compare the obtained chemical shifts between GAUSSIAN03 and GAUSSIAN98 program calculations. Considering to the chemical shifts in gas phase by using GAUSSIAN98 and GAUSSIAN03 programs, they do not show significant difference. Differently to the calculations in IEF-PCM solvation model, <sup>1</sup>H-NMR chemical shifts calculated by GAUSSIAN98 program with DMSO model gives worse SD values (excluded H23 = 2.32, included H23 = 2.45) comparing to the calculations in gas (excluded H23 = 0.19, included H23 = 0.96), but calculations by using GAUSSIAN03 show a little different shifts and SDs ( gas: excluded H23 = 0.21, included H23 = 0.97 and solvent model: excluded H23 = 0.34, included H23 = 0.84) as shown in Table 15. From the results it is found that the chemical shift of H23 in DMSO calculated by GAUSSIAN03 shows a better agreement ( $\delta = 7.09$  ppm) to the experimental data ( $\delta = 8.86$  ppm) comparing to the results from gas calculations and GAUSSIAN98 program. That means GAUSSIAN03 program calculations in solvation model can give better <sup>1</sup>H-NMR chemical shifts of H23 which is an acid proton and shows poor shifts in gas phase calculations and in GAUSSIAN98 program calculations.

For in chloroform calculations study, data in Table 16, it shows similar results that SD values (excluded H23 = 1.77, included H23 = 1.80), of proton shifts calculating by GAUSSIAN98 program were not improved from gas phase calculations. However the H23 calculated chemical shifts from GAUSSIAN03 program in chloroform model ( $\delta = 6.88$  ppm) gives better result than in gas calculation ( $\delta = 6.43$  ppm) comparing to the experiment shifts ( $\delta = 8.69$  ppm)

**Table 15** Comparison of experimental, GAUSSIAN98 (G98) and GAUSSIAN03 (G03) calculated <sup>1</sup>H-NMR chemical shifts (ppm) calculated at B3LYP/6-311++G\*\*//B3LYP/6-31G\*\* level with DMSO IEF-PCM solvation models.

<sup>1</sup> H-NMR	Expt. DMSO- <i>d</i> 6	G98 DMSO	G98 Gas	G03 DMSO	G03 Gas
21 H	8.06	7.49	8.41	8.59	8.39
22 H	7.04	9.13	7.01	7.56	7.05
23 H	9.86	6.17	6.46	7.09	6.43
24 H	8.00	2.60	8.37	8.63	8.46
25 H	7.17	10.05	7.05	7.51	7.03
26 H	8.50	9.39	8.75	8.98	8.71
27 H	2.32	1.70	2.20	2.36	2.17
28 H	2.32	-0.19	2.18	2.27	2.10
29 H	2.32	0.20	2.33	2.33	2.33
30 H	3.61	0.83	3.81	3.80	3.82
31 H	0.33	1.16	0.34	0.46	0.36
32 H	0.86	1.23	0.93	0.98	0.90
33 H	0.86	2.08	0.94	1.02	0.95
34 H	0.33	0.99	0.41	0.48	0.42
SD <sup>a</sup>		2.32	0.19	0.34	0.21
SD <sup>b</sup>		2.45	0.96	0.84	0.97

<sup>a</sup> Standard deviation (SD) =  $[\sum(x_{\text{Cal.}} - x_{\text{Expt.}})^2 / n - 1]^{1/2}$ , excluded H23

<sup>b</sup> Standard deviation (SD) =  $[\sum(x_{\text{Cal.}} - x_{\text{Expt.}})^2 / n - 1]^{1/2}$ , included H23

**Table 16** Comparison of experimental, GAUSSIAN98 (G98) and GAUSSIAN03 (G03) calculated  $^1\text{H}$ -NMR chemical shifts (ppm) calculated at B3LYP/6-311++G\*\*//B3LYP/6-31G\*\* level with chloroform IEF-PCM solvation models.

$^1\text{H}$ - NMR	Expt. CDCl <sub>3</sub>	G98 CHCl <sub>3</sub>	G98 Gas	G03 CHCl <sub>3</sub>	G03 Gas
21 H	8.16	7.82	8.41	8.53	8.39
22 H	6.94	8.46	7.01	7.40	7.05
23 H	8.69	6.52	6.46	6.88	6.43
24 H	8.11	3.69	8.37	8.58	8.46
25 H	7.07	9.13	7.05	7.36	7.03
26 H	8.54	9.21	8.75	8.90	8.71
27 H	2.41	1.68	2.20	2.30	2.17
28 H	2.41	0.91	2.18	2.22	2.10
29 H	2.41	0.75	2.33	2.33	2.33
30 H	3.77	1.71	3.81	3.84	3.82
31 H	0.50	1.17	0.34	0.42	0.36
32 H	1.00	1.17	0.93	0.95	0.90
33 H	1.00	1.73	0.94	1.00	0.95
34 H	0.50	0.74	0.41	0.46	0.42
SD <sup>a</sup>		1.77	0.17	0.27	0.19
SD <sup>b</sup>		1.80	0.64	0.56	0.65

<sup>a</sup> Standard deviation (SD) =  $[\sum(x_{\text{Cal.}} - x_{\text{Expt.}})^2 / n - 1]^{1/2}$ , excluded H23

<sup>b</sup> Standard deviation (SD) =  $[\sum(x_{\text{Cal.}} - x_{\text{Expt.}})^2 / n - 1]^{1/2}$ , included H23

**Table 17** Comparison of experimental, GAUSSIAN98 (G98) and GAUSSIAN03 (G03) calculated  $^{13}\text{C}$ -NMR chemical shifts (ppm) calculated at B3LYP/6-311++G\*\*//B3LYP/6-31G\*\* level with DMSO IEF-PCM solvation models.

$^{13}\text{C}$ - NMR	Expt.				
	DMSO- <i>d</i> 6	G98 DMSO	G98 Gas	G03 DMSO	G03 Gas
2 C	140.73	144.70	150.90	152.22	150.82
3 C	120.91	110.91	126.38	128.80	126.45
4 C	140.01	137.72	143.00	146.99	142.65
6 C	167.02	180.53	173.95	176.74	173.75
7 C	143.59	142.64	148.08	149.39	148.15
8 C	119.35	120.17	123.04	124.88	122.88
9 C	151.33	161.43	159.68	161.83	159.61
12 C	154.20	166.78	161.67	162.27	162.10
13 C	124.92	130.00	133.92	135.13	134.19
14 C	122.27	125.83	126.13	126.81	126.07
15 C	159.99	185.10	168.65	169.83	168.84
16 C	17.57	-7.33	19.71	19.73	19.65
17 C	29.29	34.73	35.45	35.64	35.56
18 C	8.52	21.48	13.36	13.24	13.39
19 C	8.75	18.21	12.89	12.57	12.74
SD <sup>a</sup>		12.37	6.57	7.93	6.61

$$^a \text{Standard deviation (SD)} = [\sum(x_{\text{Cal.}} - x_{\text{Expt.}})^2 / n - 1]^{1/2}$$

**Table 18** Comparison of experimental, GAUSSIAN98 (G98) and GAUSSIAN03 (G03) calculated  $^{13}\text{C}$ -NMR chemical shifts (ppm) calculated at B3LYP/6-311++G\*\*//B3LYP/6-31G\*\* level with chloroform IEF-PCM solvation models.

$^{13}\text{C}$ -NMR	Expt. $\text{CDCl}_3$	G98 $\text{CHCl}_3$	G98 Gas	G03 $\text{CHCl}_3$	G03 Gas
2 C	140.36	146.93	150.90	151.87	150.82
3 C	120.22	116.23	126.38	128.04	126.45
4 C	139.47	139.91	143.00	145.71	142.65
6 C	168.85	179.74	173.95	175.96	173.75
7 C	144.31	142.58	148.08	148.99	148.15
8 C	118.97	121.16	123.04	124.21	122.88
9 C	152.10	160.90	159.68	161.22	159.61
12 C	153.95	165.55	161.67	162.24	162.10
13 C	124.90	132.45	133.92	134.76	134.19
14 C	122.08	125.15	126.13	126.53	126.07
15 C	160.55	181.35	168.65	169.58	168.84
16 C	17.80	0.87	19.71	19.70	19.65
17 C	29.61	35.12	35.45	35.59	35.56
18 C	8.82	19.43	13.36	13.26	13.39
19 C	9.11	17.09	12.89	12.60	12.74
SD <sup>a</sup>		9.96	6.39	7.34	6.43

$$^a \text{Standard deviation (SD)} = [\sum(\text{X}_{\text{Cal.}} - \text{X}_{\text{Expt.}})^2 / (n-1)]^{1/2}$$

Considering to the calculated  $^{13}\text{C}$ -NMR chemical shifts in Table 17 and 18, DMSO and chloroform solvation model calculations show similar results that SD values from GAUSSIAN98 (DMSO: SD = 12.37, chloroform: SD = 9.96) and GAUSSIAN03 programs (DMSO: SD = 7.93, chloroform: SD = 7.34) calculations are not better than in gas calculations (**DMSO** G98: SD = 6.57, G03: SD = 6.11 and **CHCl<sub>3</sub>** G98: SD = 6.93, G03: SD = 6.43). However the SD values from GAUSSIAN03 programs are still better than the ones from GAUSSIAN98 programs.

**Table 19** Comparison of experimental GAUSSIAN98 (G98) and GAUSSIAN03 (G03) calculated  $^{15}\text{N}$ -NMR chemical shifts (ppm) calculated at B3LYP/6-311++G\*\*//B3LYP/6-31G\*\* level in gas phase and DMSO IEF-PCM solvation models.

Chemical shifts $\delta$ (ppm) in DMSO									
$^{15}\text{N}$ - NMR	Expt.	G98 DMSO	residual	G98 Gas	residual	G03 DMSO	residual	G03Gas	residual
1 N	-91.6	-83.7	7.9	-85.3	-6.3	-108.5	16.9	-85.6	-6.0
5 N	-252.3	-288.6	36.3	-265.9	13.6	-272.7	20.4	-265.5	13.2
10 N	-89.6	-85.6	-4.0	-85.3	-4.3	-107.6	18.0	-88.0	-1.6
11 N	-269.4	-273.9	4.5	-268.5	-0.9	-280.8	11.4	-268.640	-0.8

**Table 20** Comparison of experimental GAUSSIAN98 (G98) and GAUSSIAN03 (G03) calculated  $^{15}\text{N}$ -NMR chemical shifts (ppm) calculated at B3LYP/6-311++G\*\*//B3LYP/6-31G\*\* level in gas phase and chloroform IEF-PCM solvation models.

Chemical shifts $\delta$ (ppm) in chloroform									
$^{15}\text{N}$ - NMR	Expt.	G98 Chloroform	residual	G98 Gas	residual	G03 Chloroform	residual	G03 Gas	residual
1 N	-91.1	-84.5	-6.6	-85.3	-5.8	-101.7	10.6	-85.6	-5.5
5 N	-248.6	-275.3	26.75	-265.9	17.3	-271.0	22.4	-265.5	16.9
10 N	-86.3	-85.6	-0.68	-85.3	-1.0	-101.8	15.5	-88.0	1.7
11 N	-264.4	-271.3	6.87	-268.5	4.1	-277.5	13.1	-268.6	4.2

As shown in Tables 19 and 20, all the calculated  $^{15}\text{N}$  chemical shifts in solvent model calculated by GAUSSIAN03 programs and experimental shifts give underestimate data, but the others show the mix of underestimate and overestimate results.

From all the results, it is supported that IEF-PCM version in GAUSSIAN03 program can be used to model solvents for predicting  $^1\text{H}$ ,  $^{13}\text{C}$  and  $^{15}\text{N}$ -NMR chemical shifts of nevirapine and it shows better results of the H23  $^1\text{H}$ -NMR chemical shift which fails in gas phase calculations and in IEF-PCM version in GAUSSIAN098 program. For the next steps of study, all the calculations would be performed by GAUSSIAN03 programs.

**Table 21** Comparison of the selected torsion angles of nevirapine, obtained by different methods and compared to experimental X-ray crystallographic<sup>a</sup> data by GAUSSIAN03

X-ray	B3LYP/6-311++G**//					
	B3LYP/6-31G**			B3LYP/6-31G**		
	Gas	DMSO	Chloroform	DMSO// Gas	Chloroform// Gas	
Torsion angle (deg)						
<b>O20-C6-C14-C7</b>	<b>30.0</b>	<b>21.2</b>	<b>27.8</b>	<b>26.5</b>	<b>21.2</b>	<b>21.2</b>
C12-N11-C17-C19	68.7	71.2	71.9	72.1	71.2	71.2
C12-N11-C17-C18	136.8	139.9	140.3	140.6	139.9	139.9
C14-C15-N11-C17	168.3	159.9	156.9	157.7	159.9	160.0
C13-C12-N11-C17	200.1	205.4	207.4	206.3	205.4	205.4
<b>C15-N11-C17-C19</b>	<b>208.5</b>	<b>217.4</b>	<b>217.0</b>	<b>217.2</b>	<b>217.4</b>	<b>217.4</b>
C15-N11-C17-C18	276.6	286.1	285.5	285.8	286.1	286.1
C6-N5-C13-C14	144.4	134.8	133.7	134.9	134.8	134.8
N5-C6-C14-C7	212.9	201.1	207.2	205.8	201.1	201.0
C15-N11-C12-N1	238.8	238.0	241.7	240.2	238.0	238.0
C12-N11-C15-N10	126.7	127.9	124.1	124.9	127.9	127.9
SD <sup>b</sup>		7.7	7.2	7.0	7.7	7.7

<sup>a</sup> Data obtained resolution of 2.2 Å (Ren *et al.*, 1995)

<sup>b</sup> Standard deviation (SD) =  $[\sum(x_{\text{Cal.}} - x_{\text{Expt.}})^2 / n - 1]^{1/2}$

The geometry of nevirapine with different models and methods were compared and shown in Table 21. At B3LYP/6-31G\*\* level of optimization, some selected torsion angles were investigated. It was found that the optimized geometries in gas and in solvents (DMSO and chloroform) are little different except at O20-C6-C14-C7 torsion angle which has oxygen atom involved shows significant different. The C15-N11-C17-C19 torsion angle,  $\alpha$  angle, does not change and shows about  $\alpha = 217^\circ$ . The geometries of nevirapine from B3LYP/6-311++G\*\*(Solvent)//B3LYP/6-31G\*\*(Gas) level of calculations in DMSO and chloroform model are the same from

B3LYP/6-31G\*\* optimized calculations in gas. That means single point calculation in solvent model does not change the geometry from the B3LYP/6-31G\*\* optimized one.

**Table 22** Comparison of experimental and calculated  $^1\text{H}$ -NMR chemical shifts (ppm) calculated at B3LYP/6-311++G\*\*//B3LYP/6-31G\*\* level with DMSO IEF-PCM solvation models.

$^1\text{H}$ - NMR	Expt. DMSO- <i>d</i> 6	Gas//gas	DMSO//gas	DMSO//DMSO	Gas//DMSO
21 H	8.06	8.39	8.59	8.68	8.47
<b>22 H</b>	<b>7.04</b>	<b>7.05</b>	<b>7.56</b>	<b>7.63</b>	<b>7.11</b>
<b>23 H</b>	<b>9.86</b>	<b>6.43</b>	<b>7.09</b>	<b>7.60</b>	<b>6.63</b>
24 H	8.00	8.46	8.63	8.53	8.30
<b>25 H</b>	<b>7.17</b>	<b>7.03</b>	<b>7.51</b>	<b>7.60</b>	<b>7.11</b>
26 H	8.50	8.71	8.98	9.00	8.73
27 H	2.32	2.17	2.36	2.40	2.20
28 H	2.32	2.10	2.27	2.22	2.06
29 H	2.32	2.33	2.33	2.35	2.37
30 H	3.61	3.82	3.80	3.94	3.96
31 H	0.33	0.36	0.46	0.48	0.38
32 H	0.86	0.90	0.98	0.96	0.87
33 H	0.86	0.95	1.02	0.98	0.90
34 H	0.33	0.42	0.48	0.49	0.44
SD <sup>a</sup>		0.21	0.34	0.37	0.21
SD <sup>b</sup>		0.97	0.84	0.72	0.92

<sup>a</sup> Standard deviation (SD) =  $[\sum(x_{\text{Cal.}} - x_{\text{Expt.}})^2 / n - 1]^{1/2}$ , excluded H23

<sup>b</sup> Standard deviation (SD) =  $[\sum(x_{\text{Cal.}} - x_{\text{Expt.}})^2 / n - 1]^{1/2}$ , included H23

**Table 23** Comparison of experimental and calculated  $^1\text{H-NMR}$  chemical shifts (ppm) calculated at B3LYP/6-311++G\*\*//B3LYP/6-31G\*\* level with chloroform IEF-PCM solvation models.

$^1\text{H-NMR}$	Expt.				
	$\text{CDCl}_3$	Gas//gas	$\text{CHCl}_3$ //gas	$\text{CHCl}_3$ // $\text{CHCl}_3$	Gas// $\text{CHCl}_3$
21 H	8.16	8.39	8.53	8.59	8.45
<b>22 H</b>	<b>6.94</b>	<b>7.05</b>	<b>7.40</b>	<b>7.44</b>	<b>7.09</b>
<b>23 H</b>	<b>8.69</b>	<b>6.43</b>	<b>6.88</b>	<b>7.12</b>	<b>6.53</b>
24 H	8.11	8.46	8.58	8.48	8.34
<b>25 H</b>	<b>7.07</b>	<b>7.03</b>	<b>7.36</b>	<b>7.42</b>	<b>7.08</b>
26 H	8.54	8.71	8.90	8.92	8.73
27 H	2.41	2.17	2.30	2.32	2.18
28 H	2.41	2.10	2.22	2.18	2.07
29 H	2.41	2.33	2.33	2.34	2.34
30 H	3.77	3.82	3.84	3.94	3.93
31 H	0.50	0.36	0.42	0.43	0.38
32 H	1.00	0.90	0.95	0.95	0.89
33 H	1.00	0.95	1.00	0.96	0.91
34 H	0.50	0.42	0.46	0.46	0.43
$\text{SD}^{\text{a}}$		0.19	0.27	0.28	0.19
$\text{SD}^{\text{b}}$		0.65	0.56	0.51	0.63

<sup>a</sup> Standard deviation (SD) =  $[\sum(x_{\text{Cal.}} - x_{\text{Expt.}})^2 / n - 1]^{1/2}$ , excluded H23

<sup>b</sup> Standard deviation (SD) =  $[\sum(x_{\text{Cal.}} - x_{\text{Expt.}})^2 / n - 1]^{1/2}$ , included H23

To study the effect of solvent optimization, the comparison between experimental and calculated  $^1\text{H}$ ,  $^{13}\text{C}$  and  $^{15}\text{N}$ -NMR chemical shifts were compared. The results of NMR calculations by different gas and solvent models of calculations, B3LYP/6-311++G\*\* (gas or solvent)//B3LYP/6-31G\*\* (gas or solvent), are shown in Tables 22-27. As it has been discussed that the optimized geometries in gas and in solvents (DMSO and chloroform) are not much different, the shifts of gas//gas and gas//solvent calculations give similar SDs. Similarly to the SDs of solvent//gas and solvent // solvent calculations that the SDs are not much different. The surprised results are the  $^1\text{H}$ -NMR chemical shifts of H23. Both calculated  $^1\text{H}$ -NMR chemical shifts of H23 in DMSO and chloroform show better agreement to the experimental shifts, solvent//solvent > solvent//gas > gas//solvent > gas//gas. The best shifts of H23 from solvent//solvent calculations in DMSO and chloroform are 7.60 and 7.12 ppm which are 1.17 ppm and 0.69 ppm more in low-field shift from gas phase calculations respectively. The results from solvent//solvent calculations are closer to the experimental shifts (9.86 and 8.69 ppm for DMSO and chloroform respectively). It means to predict the chemical shifts of H23 which is an active proton and difficult to calculate can be taken care more by using IEF-PCM model even though the shifts are still about 2-3 ppm underestimated. The H22 and H25 proton chemical shifts seem to be inaccurate as they are more overestimated in IEF-PCM model calculations. It shows that it is something more to be concerned and still needed to improve for more correct prediction.

**Table 24** Comparison of experimental and calculated  $^{13}\text{C}$ -NMR chemical shifts (ppm) calculated at B3LYP/6-311++G\*\*//B3LYP/6-31G\*\* level with DMSO IEF-PCM solvation models.

$^{13}\text{C}$ -NMR	Expt.				
	DMSO- <i>d</i> 6	Gas//gas	DMSO//gas	DMSO//DMSO	Gas//DMSO
2 C	140.73	150.82	152.22	153.64	152.27
3 C	120.91	126.45	128.80	129.18	126.74
4 C	140.01	142.65	146.99	150.15	145.77
6 C	167.02	173.75	176.74	177.97	175.00
7 C	143.59	148.15	149.39	149.06	147.58
8 C	119.35	122.88	124.88	125.84	123.76
9 C	151.33	159.61	161.83	161.89	159.71
12 C	154.20	162.10	162.27	164.89	164.88
13 C	124.92	134.19	135.13	134.95	133.86
14 C	122.27	126.07	126.81	128.55	127.76
15 C	159.99	168.84	169.83	170.51	169.45
16 C	17.57	19.65	19.73	20.23	20.13
17 C	29.29	35.56	35.64	34.46	34.42
18 C	8.52	13.39	13.24	12.51	12.67
19 C	8.75	12.74	12.57	12.04	12.24
SD <sup>a</sup>		6.61	7.93	8.73	7.30

$$^a \text{Standard deviation (SD)} = [\sum(x_{\text{Cal.}} - x_{\text{Expt.}})^2 / n - 1]^{1/2}$$

**Table 25** Comparison of experimental and calculated  $^{13}\text{C}$ -NMR chemical shifts (ppm) calculated at B3LYP/6-311++G\*\*//B3LYP/6-31G\*\* level with chloroform IEF-PCM solvation models.

$^{13}\text{C}$ -NMR	Expt.				
	$\text{CDCl}_3$	Gas//gas	$\text{CHCl}_3$ //gas	$\text{CHCl}_3$ // $\text{CHCl}_3$	Gas// $\text{CHCl}_3$
2 C	140.36	150.82	151.87	152.80	151.77
3 C	120.22	126.45	128.04	128.23	126.61
4 C	139.47	142.65	145.71	147.77	144.68
6 C	168.85	173.75	175.96	176.78	174.56
7 C	144.31	148.15	148.99	148.68	147.73
8 C	118.97	122.88	124.21	124.94	123.57
9 C	152.10	159.61	161.22	161.30	159.71
12 C	153.95	162.10	162.24	164.09	163.99
13 C	124.90	134.19	134.76	134.55	133.94
14 C	122.08	126.07	126.53	127.92	127.43
15 C	160.55	168.84	169.58	169.96	169.19
16 C	17.80	19.65	19.70	20.00	19.92
17 C	29.61	35.56	35.59	34.81	34.80
18 C	8.82	13.39	13.26	12.75	12.87
19 C	9.11	12.74	12.60	12.33	12.46
SD <sup>a</sup>		6.43	7.34	7.87	6.90

$$^a \text{Standard deviation (SD)} = [\sum(x_{\text{Cal.}} - x_{\text{Expt.}})^2 / n - 1]^{1/2}$$

**Table 26** Comparison of experimental and calculated  $^{15}\text{N}$ -NMR chemical shifts (ppm) calculated at B3LYP/6-311++G\*\*//B3LYP/6-31G\*\* level with DMSO IEF-PCM solvation models.

$^{15}\text{N}$ - NMR	Chemical shifts $\delta$ (ppm) in DMSO								
	Expt.	Gas//gas	residual	DMSO//gas	residual	DMSO//DMSO	residual	Gas//DMSO	residual
1 N	-91.6	-85.6	-6.0	-108.5	16.9	-104.5	12.9	-85.5	-6.1
5 N	-252.3	-265.5	13.2	-272.7	20.4	-269.5	17.2	-268.2	15.9
10 N	-89.6	-88.0	-1.6	-107.6	18.0	-103.5	13.9	-87.4	-2.2
11 N	-269.4	-268.6	-0.80	-280.8	11.4	-281.8	12.4	-274.2	4.8

**Table 27** Comparison of experimental and calculated  $^{15}\text{N}$ -NMR chemical shifts (ppm) calculated at B3LYP/6-311++G\*\*//B3LYP/6-31G\*\* level with chloroform IEF-PCM solvation models

$^{15}\text{N}$ - NMR	Chemical shifts $\delta$ (ppm) in chloroform								
	Expt.	Gas//gas	residual	$\text{CHCl}_3$ //gas	residual	$\text{CHCl}_3$ // $\text{CHCl}_3$	residual	Gas// $\text{CHCl}_3$	residual
1 N	-91.1	-85.6	-5.5	-101.7	10.6	-102.3	11.2	-85.9	-5.1
5 N	-248.6	-265.5	16.9	-271.0	22.4	-272.2	23.6	-267.4	18.8
10 N	-86.3	-88.0	1.7	-101.8	15.5	-101.7	15.4	-87.4	1.1
11 N	-264.4	-268.6	4.2	-277.5	13.1	-281.3	16.9	-272.5	8.1

#### **4. $^1\text{H}$ -NMR chemical shift improvement : MD-QM approach**

Even though IEF-PCM model generally provides long-range electrostatic interactions, in this case of study, the  $^1\text{H}$ -NMR chemical shifts of H23 still cannot be predicted correctly in the solvation model. It is an idea that supermolecule calculations involving a solute surrounded by a number of explicitly treated solvent molecules can represent short-range interactions. To include short-range interactions to the model of calculations, molecular dynamics simulations (MD) were used to prepare model structures for NMR calculations of nevirapine with solvent molecules. The combination of the two approaches when coupled to accurate quantum mechanical methods should give an effective computational tool to include solvent effects into nuclear shielding calculations.

##### **4.1 Radial Distribution Functions and Selection of Nevirapine-DMSO Structures**

During the MD simulations, the root mean square deviation (RMSD) of heavy atoms in nevirapine from the starting geometry and the total energy of the whole system were observed. The RMSD versus simulation time is shown in Figure 9a. There is little fluctuation indicating that nevirapine is stable in this MD simulation. The total energy fluctuation as a function of time is shown in Figure 9b. After the 50ps equilibration period, the energy became stable within 20ps indicating the thermodynamic properties of the modelled system were well equilibrated.

From the RDFs of the four different atom types in DMSO around the acidic proton, shown in Figure 10, it can be seen that the oxygen distribution gives the sharpest peak closest to the proton. This gives the first shell of solvent atoms around the proton as consisting of oxygen from DMSO at an average distance of 1.9 Å. Integrating the area under the peak, to the minimum at 3.0 Å, gives a total of one atom in this shell. This shows the hydrogen bonding between the two molecules expected. The other RDFs also support this as the sulfur distribution shows the next most distinctive peak at an average distance of 3.1 Å from the proton. Its broader spread showing that the sulfur is less constrained compared to the oxygen, but there is still

only one atom within a 3.6 Å shell. The DMSO carbon and hydrogen atom distributions show only small, broad peaks due their less constrained positions at the far ends of the molecule, and also from the passing of methyl groups of other unattached solvent molecules through the solvation shell volume.

From these results the cut-off for the discrete model used in quantum calculations was set to 3.0 Å. This corresponds to the radius of the shell that complete encloses the nearest solvent atoms to the acidic proton, as given by the minimum after the peak of the oxygen RDF. In the sample set of snapshots, any molecules that were even partial inside this cut-off distance were included in the model.

Figure 11 shows examples of the nevirapine-DMSO models from four of the snapshots used in the quantum calculations. Only the single solvent molecule within the 3.0 Å cut-off is shown. The other 181 molecules have been removed for clarity, and were not further used.

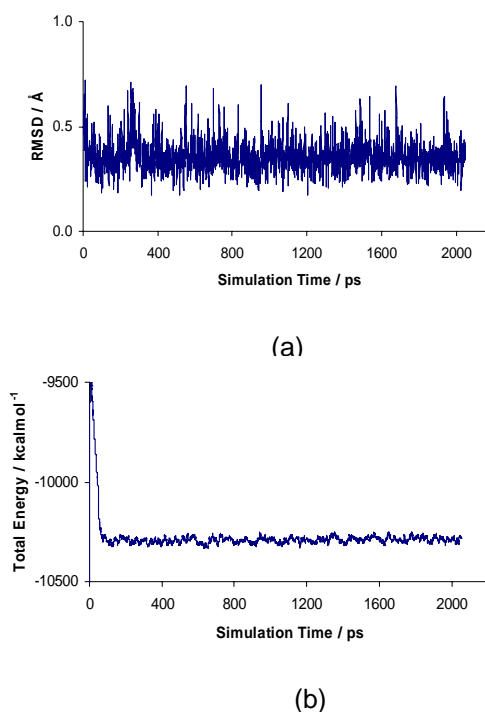


**Figure 9** (a) RMSD (Å) and (b) total energy (kcalmol<sup>-1</sup>) of nevirapine in DMSO from MD simulations.

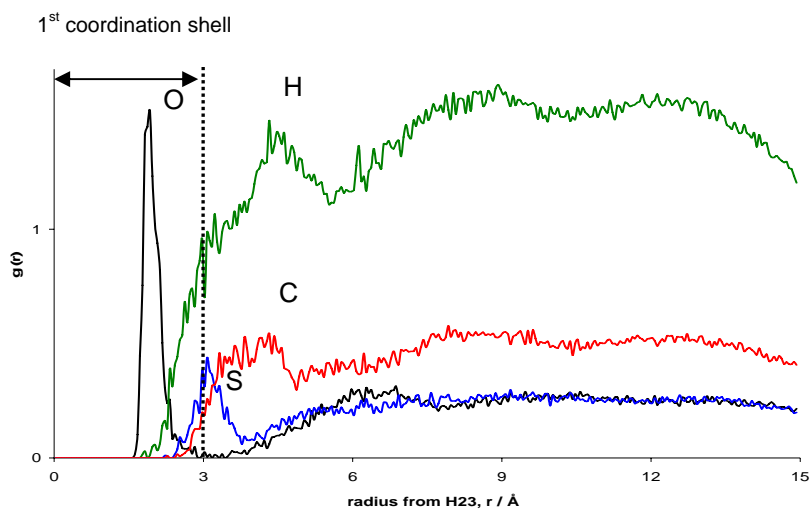


**Figure 10** RDFs for the atoms of DMSO relative to the acidic proton H23 of nevirapine. By integration 1<sup>st</sup> coordination shell contains one DMSO oxygen atom. Hence one DMSO molecule is bonded to the proton.

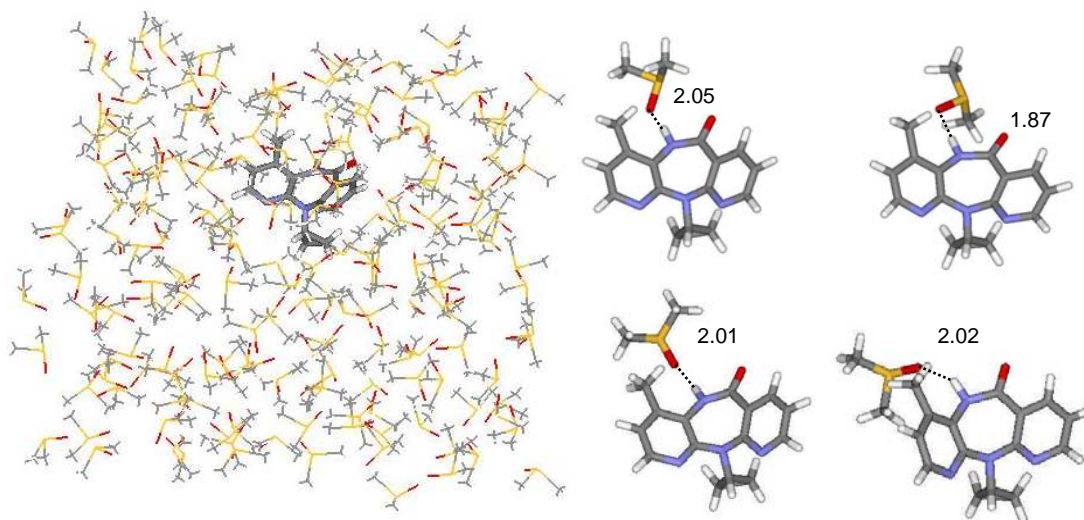


**Figure 11** A snapshot of nevirapine in a box of 182 DMSO molecules is shown on the left. Four examples of the nevirapine-DMSO model cropped from snapshots taken during MD simulations, used in ONIOM2 and NMR calculations, are shown on the right. The numbers indicate the distance between the acidic proton H23 and the oxygen of DMSO in Å.

A sample set of nevirapine-DMSO structures was generated from snapshots of the system taken every 100 ps during the last 1ns of the production period. Each nevirapine-DMSO structure was used for NMR calculations at B3LYP/6-311++G\*\*//B3LYP/6-31G\*\* level in gas phase and DMSO IEF-PCM model as in the previous modelling work. Finally NMR shifts from each snapshot used were averaged.

#### **4.2 NMR calculations of obtained nevirapine-DMSO structures from MD simulations**

As shown in Table 28 comparing between previous simple nevirapine calculations in gas phase and with DMSO IEF-PCM model, the shift of H23 is approximately 0.5 ppm in the lower field, which is a little closer to the experimental result, but the standard deviation is larger as most of the other chemical shifts are overestimated. This shows that the IEF-PCM model cannot properly model the H23 chemical shift in this system. The H23 chemical shift, using the MD approach to generate nevirapine-DMSO structures for NMR calculations in gas phase, is 10.93 ppm which is approximately 1.1 ppm in the lower field than the measured shift of 9.86 ppm, and 4.5 ppm lower than that predicted by the previous simple nevirapine model. Figure 12 shows the plots of experimental and calculated chemical shifts.

It can be concluded that in this system, short range interaction effects, especially H-bond effects, are very important in understanding the acidic proton chemical shifts as these strongly influence the electronic environment of this proton. The discrete model is effective in dealing with these effects. Looking at the short and long range interactions separately, the combined IEF-PCM method with NMR calculations using the nevirapine-DMSO model does not show better prediction than nevirapine-DMSO model in gas phase.

These calculated  $^1\text{H}$ -NMR shifts of nevirapine were then compared to experimentally measured shifts to show the accuracy of the model used, and to show that it is an acceptable and efficient improvement over previous models.

**Table 28** Comparison of experimental and calculated  $^1\text{H}$ -NMR chemical shifts,  $\delta$  (ppm). Including standard deviations (SD)s of differences between these values.

$^1\text{H}$ - NMR	Expt. $\delta$ (ppm)	Simple NEV $\delta$ (ppm)	Simple NEV with IEF-PCM $\delta$ (ppm)	NEV-DMSO <sup>a</sup> $\delta$ (ppm)	NEV-DMSO with IEF- PCM <sup>a</sup> $\delta$ (ppm)
H21	8.06	8.39	8.59	8.33	8.54
H22	7.04	7.05	7.56	6.90	7.37
<b>H23</b>	<b>9.86</b>	<b>6.43</b>	<b>7.09</b>	<b>10.93</b>	<b>11.02</b>
H24	8.00	8.46	8.63	8.27	8.53
H25	7.17	7.03	7.51	7.04	7.56
H26	8.50	8.71	8.98	8.73	8.99
H27	2.32	2.17	2.36	2.99	2.94
H28	2.32	2.10	2.27	2.47	2.53
H29	2.32	2.33	2.33	2.29	2.41
H30	3.61	3.82	3.80	3.80	3.76
H31	0.33	0.36	0.46	0.36	0.41
H32	0.86	0.90	0.98	0.83	0.92
H33	0.86	0.95	1.02	0.86	0.95
H34	0.33	0.42	0.48	0.35	0.42
SD <sup>b</sup>		0.97	1.10	0.34	0.44

<sup>a</sup> Average values from nevirapine-DMSO models

<sup>b</sup> Standard deviation (SD) =  $[\sum(x_{\text{Cal.}} - x_{\text{Expt.}})^2 / n - 1]^{1/2}$

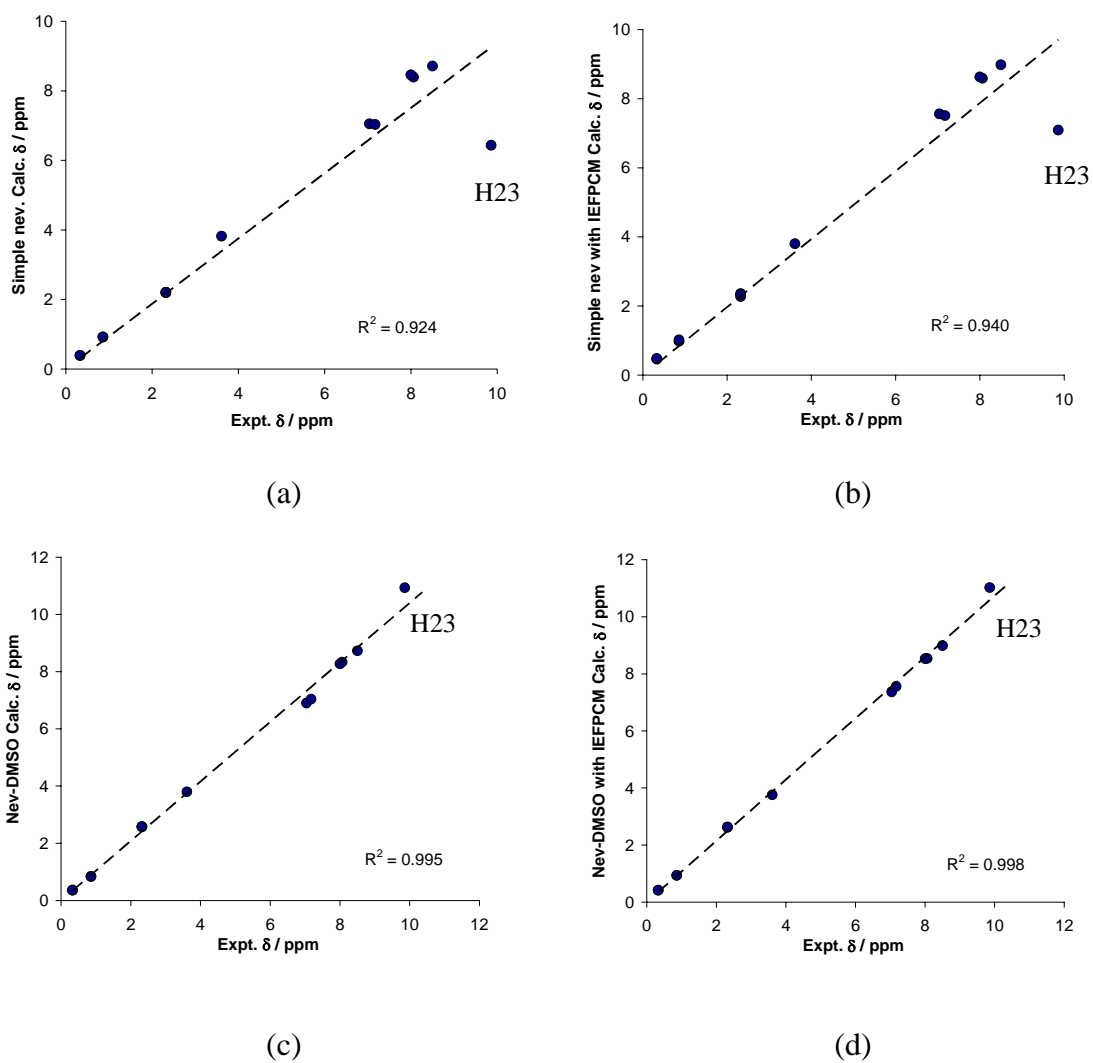


**Figure 12** Plot of (a) simple nevirapine, (b) simple nevirapine with DMSO IEF-PCM model, (c) nevirapine-DMSO and (d) nevirapine-DMSO with IEF-PCM models calculated  $^1\text{H}$  chemical shifts versus experimental chemical shifts in ppm.

ONIOM2 at the B3LYP/6-31G\*\*:<sup>PM3</sup> level was used to optimise the combined structure and at the B3LYP/6-311++G\*\*:<sup>HF/STO-3G</sup> level to calculate NMR shifts of each model taken from each snapshot in the sample set. Averaging the calculated shifts removed any transient effects on the shifts caused by the dynamic nature of solvent molecules moving around. These averaged values also compare well to measured data, with at most 0.25 ppm difference, and now also for the acidic proton as shown in Table 29. The predicted shift of 9.53 ppm is very close to the 9.86 ppm measured. The standard deviations (SD) given in the table, and the plots showing calculated shifts against measured shifts in Figure 13, show the new approach does give more accurate predictions of NMR shifts, and for all proton types.

Of additional interest are the shifts of the three methyl hydrogens H27, H28 and H29. The measured spectrum shows only a single sharp peak for at 2.32 ppm suggesting that these protons are equivalent. However, the predicted values show slight differences as in the discrete, static models used the three are not exactly equal. This is more obvious in the nevirapine-DMSO model as the bound DMSO molecule near the methyl group brings more de-shielding asymmetry to the group. Normally rotation of the methyl group averages out these values, and examination of the sample snapshots showed that this group is rotating. Averaging the predicted values for these three protons gives an average shift of 2.20 ppm for the simple nevirapine model, and 2.43 ppm for the nevirapine-DMSO model, both agreeing reasonably well with the measured value of 2.32 ppm.

In contrast, the pairs of protons H31/H34 and H32/H33 of the cyclopropyl group are each also equivalent from the measured spectrum with peaks at 0.33 ppm and 0.86 ppm respectively. The predicted shifts from both previous and current modelling suggest this equivalence as there is no significant variation. Thus modelling, with the present model especially, can show details of hydrogen electronic environments that are lost or averaged out in the dynamics of a real system. Conversely, this also shows that care must be taken to ensure that the dynamics of the system is understood and where appropriate predicted values are averaged to accurately reflect a real system.

**Table 29** Comparison of experimental and calculated  $^1\text{H-NMR}$  chemical shifts of simple nevirapine and nevirapine-DMSO model by using ONIOM2 method,  $\delta$  (ppm). Including standard deviations (SD)s of differences between these values.

$^1\text{H-NMR}$	Expt. $\delta$ (ppm)	Calc. Simple NEV $\delta$ (ppm)	Calc. NEV-DMSO <sup>a</sup> $\delta$ (ppm)
H21	8.06	8.39	8.21
H22	7.04	7.05	6.81
<b>H23</b>	<b>9.86</b>	<b>6.43</b>	<b>9.53</b>
H24	8.00	8.46	8.26
H25	7.17	7.03	6.99
H26	8.50	8.71	8.64
H27	2.32	2.17	2.65
H28	2.32	2.10	2.45
H29	2.32	2.33	2.24
H30	3.61	3.82	3.85
H31	0.33	0.36	0.34
H32	0.86	0.90	0.84
H33	0.86	0.95	0.87
H34	0.33	0.42	0.37
SD <sup>b</sup>		0.97	0.17

<sup>a</sup> Average values from nevirapine-DMSO models

<sup>b</sup> Standard deviation (SD) =  $[\sum(x_{\text{Cal.}} - x_{\text{Expt.}})^2 / n - 1]^{1/2}$

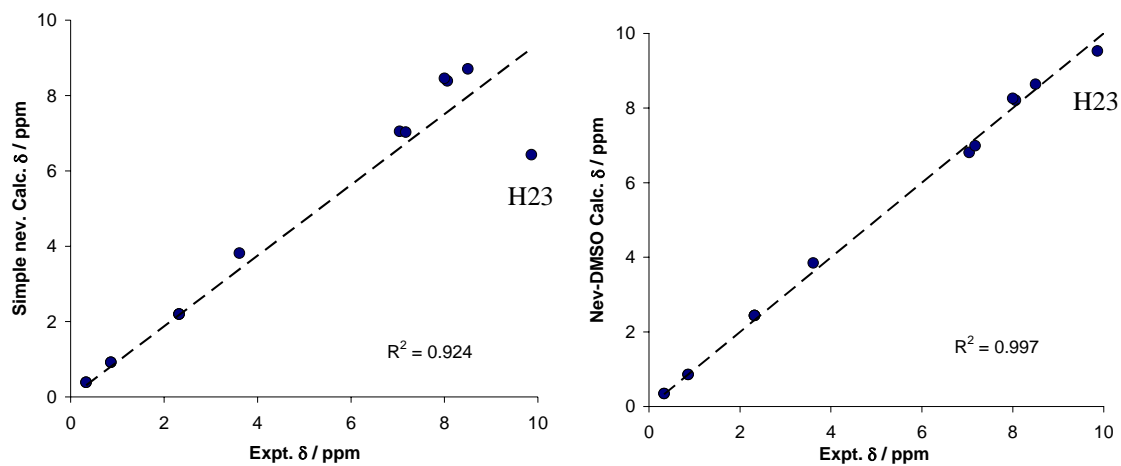


**Figure 13** Plot of (a) simple nevirapine and (b) ONIOM2 nevirapine-DMSO models calculated  $^1\text{H}$  chemical shifts versus experimental chemical shifts in ppm.

### **4.3 Radial Distribution Functions and Selection of Nevirapine-CHCl<sub>3</sub> Structures**

As it has done for nevirapine in DMSO system, RMSD of heavy atoms in nevirapine from the starting geometry and the total energy of the whole system were observed. The RMSD versus simulation time is shown in Figure 14a. There is little fluctuation indicating that nevirapine is stable in this MD simulation. The total energy fluctuation as a function of time is shown in Figure 14b. After the equilibration period, the energy became stable indicating the thermodynamic properties of the modelled system were well equilibrated. The nevirapine-CHCl<sub>3</sub> discrete model was sampled via snapshots every 200ps during the last 1ns of simulation.

From the RDFs of the three different atom types in CHCl<sub>3</sub> around the acidic proton, shown in Figure 15, it can be seen that all chloride, hydrogen and carbon distributions do not give any sharp peaks close to the proton. It means this system has no hydrogen bonds and less constrained positions. Although the CHCl<sub>3</sub> hydrogen distribution shows a little higher broad peak than the others. This was considered as the first shell of solvent atoms around the proton. Integrating the area under the peak, to the minimum at 5.1 Å, gives a total of three atoms in this shell.

From these results the cut-off for the discrete model used in quantum calculations was set to 5.1 Å. This corresponds to the radius of the shell that completely encloses the nearest solvent atoms to the acidic proton, as given by the minimum after the peak of the oxygen RDF. In the sample set of snapshots, any molecules that were even partial inside this cut-off distance were included in the model.

Figure 16 shows a snapshot of nevirapine in a box of CHCl<sub>3</sub> and Figure 17 shows examples of the nevirapine-CHCl<sub>3</sub> models from five of the snapshots used in the quantum calculations.

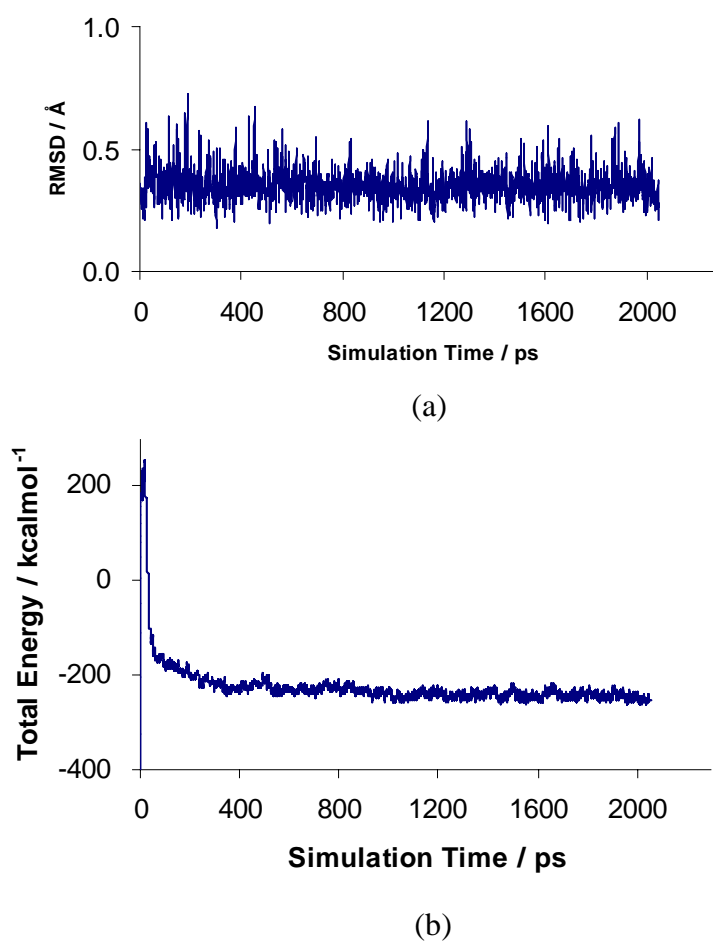


**Figure 14** (a) RMSD ( $\text{\AA}$ ) and (b) total energy ( $\text{kcalmol}^{-1}$ ) of nevirapine in chloroform from MD simulations.

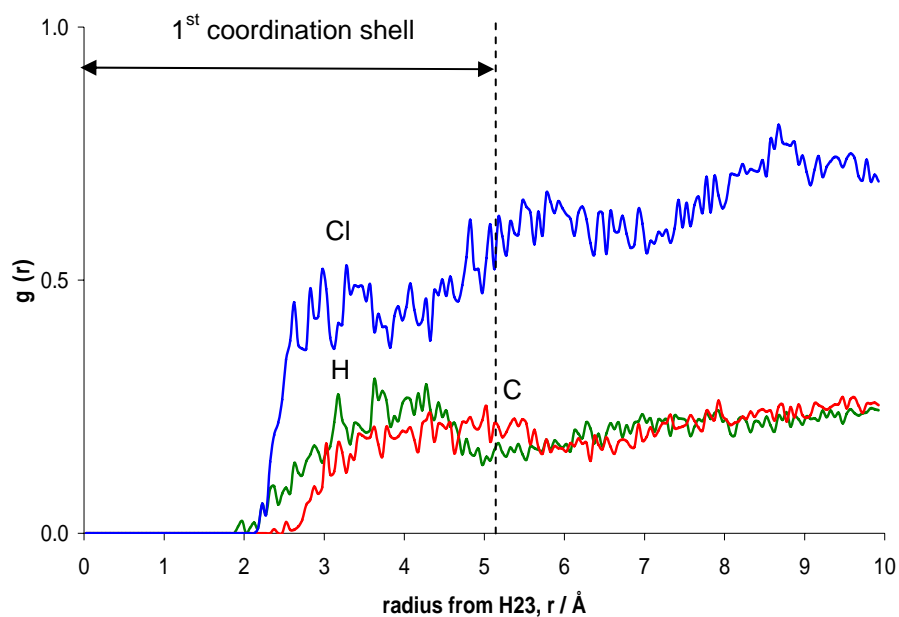


**Figure 15** RDFs for the atoms of  $\text{CHCl}_3$  relative to the acidic proton H23 of nevirapine. By integration 1<sup>st</sup> coordination shell contains three  $\text{CHCl}_3$  hydrogen atoms.

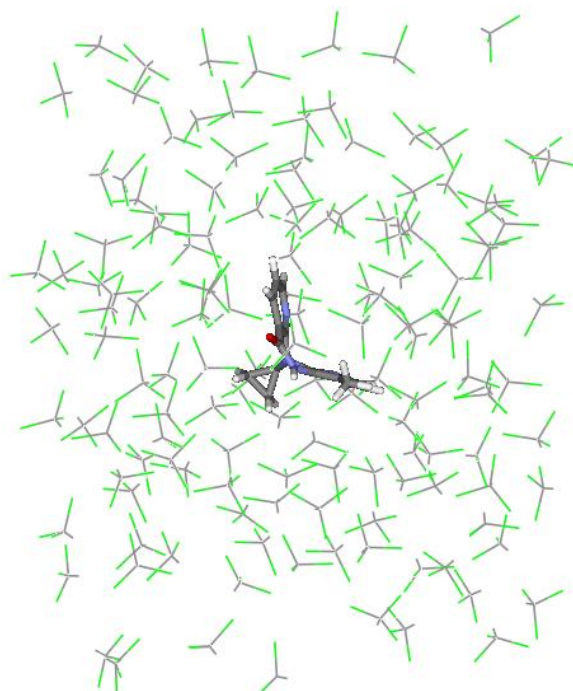


**Figure 16** A snapshot of nevirapine in a box of 141  $\text{CHCl}_3$  molecules.

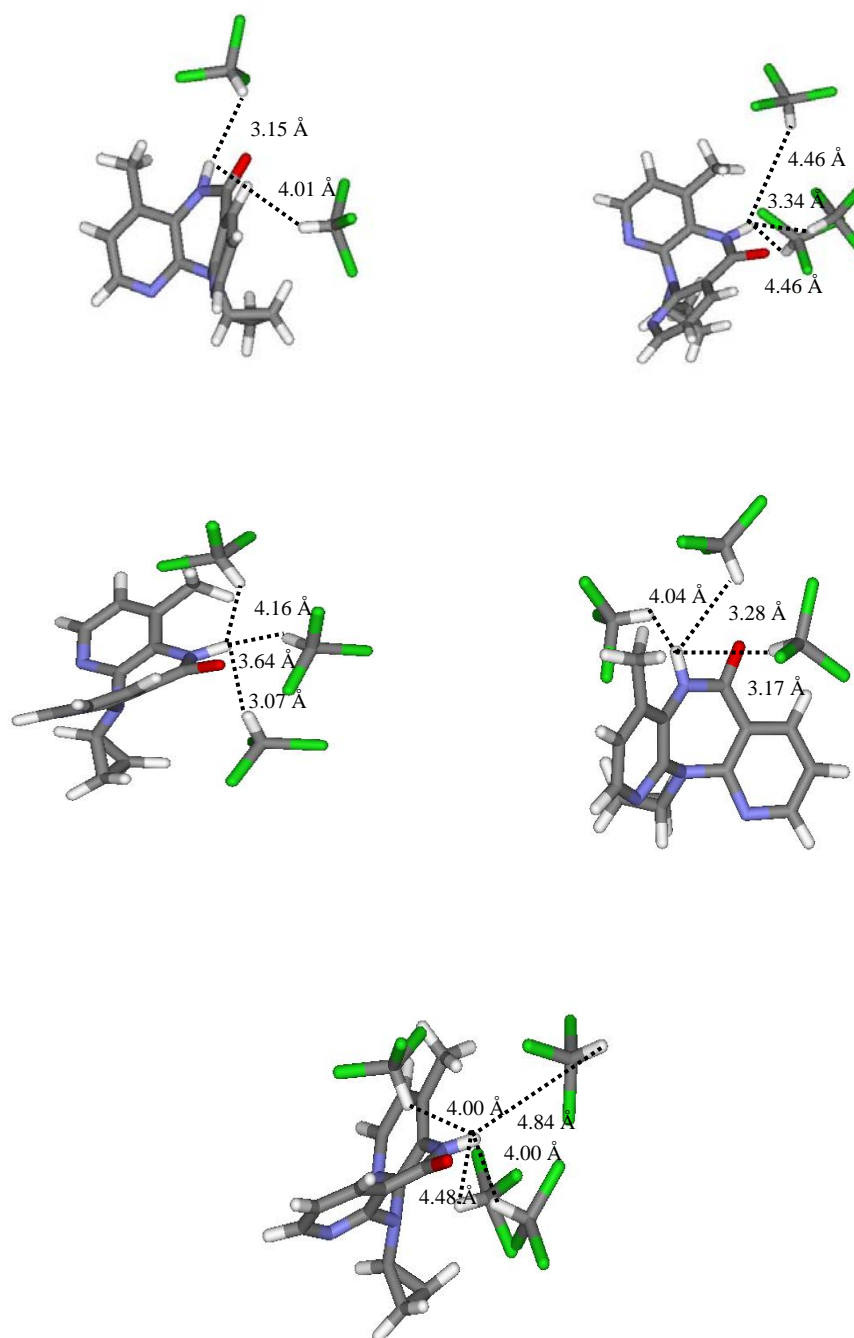


**Figure 17** Five nevirapine-DMSO models cropped from snapshots taken during from MD simulations, used in ONIOM2 and NMR calculations, are shown on the right. The numbers indicate the distance between the acidic proton H23 and the oxygen of DMSO in Å.

#### **4.4 NMR calculations of obtained nevirapine-CHCl<sub>3</sub> structures from MD simulations**

As ONIOM2 could present well results for nevirapine in DMSO system, the ONIOM2 at the B3LYP/6-31G\*\*:<sup>PM3</sup> level was used to optimise the combined structure and at the B3LYP/6-311++G\*\*:<sup>HF/STO-3G</sup> level to calculate <sup>1</sup>H-NMR shifts of each nevirapine-CHCl<sub>3</sub> model taken from each snapshot in the sample set. The averaged values compared to simple model results and measured data are shown in Table 30. The predicted shift of H23 is the same as the simple nevirapine calculations with CHCl<sub>3</sub> IEF-PCM model at 6.88 ppm and the other <sup>1</sup>H-NMR shifts are similar to the simple nevirapine calculations in gas. It shows that MD-ONIOM2 approach can reproduce the same result of H23 as calculations with CHCl<sub>3</sub> IEF-PCM model even though it still can not represent the accurate result at 8.63 ppm. Different to nevirapine in DMSO system which has strong hydrogen bond and the discrete model is effective in dealing with these effects, nevirapine in CHCl<sub>3</sub> system does not have hydrogen bond. In this case, short range interaction is less important to calculate acidic proton of nevirapine.

The measured spectrum of equivalent H27, H28 and H29 hydrogens shows only a single sharp peak for at 2.41 ppm. The predicted values show slight differences as in the discrete, static models used the three are not exactly equal. Averaging the predicted values for these three protons gives an average shift of 2.20 ppm for the simple nevirapine model, 2.28 ppm for simple nevirapine with chloroform IEF-PCM model, and 2.44 ppm for the nevirapine-CHCl<sub>3</sub> model, all agreeing reasonably with the measured value of 2.41 ppm.

The pairs of protons H31/H34 and H32/H33 of the cyclopropyl group are each also equivalent from the measured spectrum with peaks at 0.50 ppm and 1.00 ppm respectively. The average predicted values from both previous models and current modelling agree well with the measured values.

The standard deviations (SD)s given in the Table 30, and the plots showing calculated shifts against measured shifts in Figure 18.

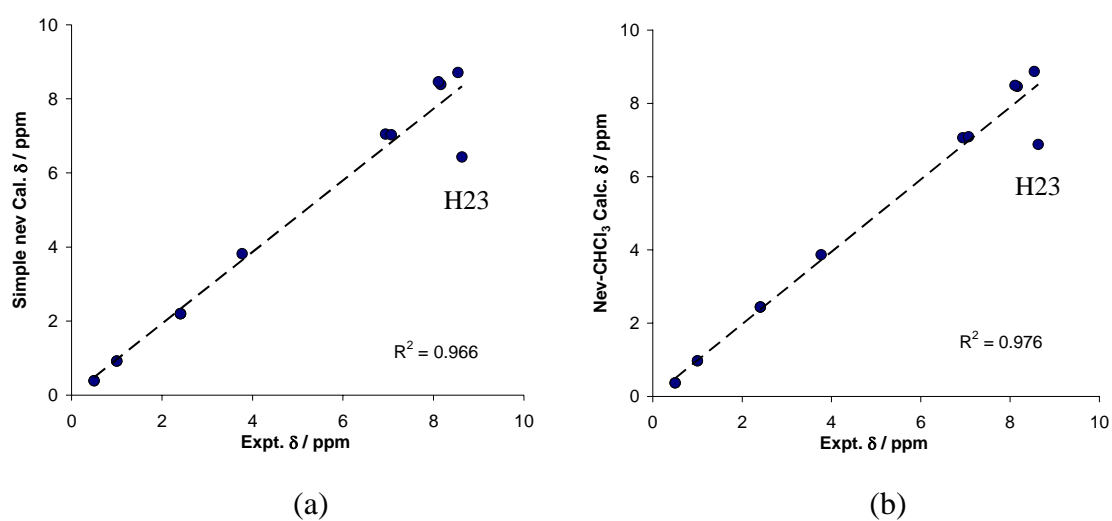


**Figure 18** Plot of (a) simple nevirapine and (b) ONIOM2 nevirapine- $\text{CHCl}_3$  models calculated  $^1\text{H}$  chemical shifts versus experimental chemical shifts in ppm.

**Table 30** Comparison of experimental and calculated  $^1\text{H-NMR}$  chemical shifts of simple nevirapine and nevirapine- $\text{CHCl}_3$  model by using ONIOM2 method,  $\delta$  (ppm). Including standard deviations (SD)s of differences between these values.

Proton	Expt.	Calc. Simple	Calc. IEF-PCM	Calc.
	$\delta$ (ppm)	NEV $\delta$ (ppm)	NEV $\delta$ (ppm)	NEV- $\text{CHCl}_3^a$ $\delta$ (ppm)
H21	8.16	8.39	8.53	8.46
H22	6.94	7.05	7.40	7.06
<b>H23</b>	<b>8.63</b>	<b>6.43</b>	<b>6.88</b>	<b>6.88</b>
H24	8.11	8.46	8.58	8.49
H25	7.07	7.03	7.36	7.09
H26	8.54	8.71	8.90	8.87
H27	2.41	2.17	2.30	2.64
H28	2.41	2.10	2.22	2.37
H29	2.41	2.33	2.33	2.32
H30	3.77	3.82	3.84	3.87
H31	0.50	0.36	0.42	0.20
H32	1.00	0.90	0.95	0.95
H33	1.00	0.95	1.00	0.98
H34	0.50	0.42	0.46	0.55
SD <sup>b</sup>		0.65	0.56	0.54

<sup>a</sup> Average values from nevirapine-  $\text{CHCl}_3$  models

<sup>b</sup> Standard deviation (SD) =  $[\sum(x_{\text{Cal.}} - x_{\text{Expt.}})^2 / n - 1]^{1/2}$

## 5. IR frequency calculations

IR frequency calculations were used to check the nevirapine structure for the simple nevirapine model and also selected discrete nevirapine-DMSO and nevirapine-CHCl<sub>3</sub> models. As Radom and Scott (Radom *et al.*, 1996) presented the scaling factors for obtaining fundamental vibrational frequencies, 0.9614, for B3LYP/6-31G\* method, in this study, the calculated IR frequencies were calculated at B3LYP/6-31G\*//B3LYP/6-31G\*\* level and corrected with 0.9614 and then compared to the experimental results. The experimental IR spectrum of nevirapine is shown in Figure 19.

Considering at simple nevirapine model calculations, the obtained spectrum is very similar to pure solid nevirapine IR experimental results. The selected IR vibrational frequencies are shown in Table 31. It shows that the calculations are correct and B3LYP /6-31G\*//B3LYP/6-31G\*\* level with 0.9614 scaling factor can be used. The interest is at N-H stretching because it was found before that for discrete nevirapine-DMSO model, short range or hydrogen bond interaction at the acidic proton is very strong and shows <sup>1</sup>H-NMR shift in the low field comparing to the simple nevirapine model. As shown in Figure 19, N-H stretching peak at about 3500 cm<sup>-1</sup> appears in simple nevirapine and nevirapine-CHCl<sub>3</sub> models but it shifts to about 3138 cm<sup>-1</sup> in nevirapine-DMSO model. This shows that the nature of H23 of nevirapine-DMSO model is different to the simple nevirapine and nevirapine-CHCl<sub>3</sub> models. In contrast, N-H stretching frequency of nevirapine-CHCl<sub>3</sub> is still at about 3500 cm<sup>-1</sup>, while the peak at 3056 cm<sup>-1</sup> is only aromatic C-H stretching. The peak at 711 cm<sup>-1</sup> is C-Cl stretching of chloroform. The IR spectra of isolated DMSO and CHCl<sub>3</sub> are shown in Figure 20. A broad peak around 3200-3600 cm<sup>-1</sup> of experimental nevirapine in DMSO spectrum can be explained by dynamics and proton exchange which occurs in this system. However moisture can be easily absorbed in DMSO solvent and it shows a broad peak around 3500 cm<sup>-1</sup> as well. The experimental IR spectra are showed in Figure 21.

**Table 31** Experimental and calculated<sup>a</sup> IR vibrational frequencies at B3LYP/6-31G\*\*//B3LYP/6-31G\*\* level of nevirapine

Expt. Nev	Frequency (cm <sup>-1</sup> )			Assignment
	Calc. Nev	Calc. Nev-DMSO	Calc. Nev-CHCl <sub>3</sub>	
1355	1343	1251	1360	C-N aromatic stretching
1383	1409	1277	1410	C-N aromatic stretching
1415	1429	1403	1401	C-H aliphatic bending
1586	1583	1582	1582	C=C aromatic stretching
1600	1586	1582	1585	C=C aromatic stretching
1649	1696	1633	1640	C=O stretching
3063	3052	3050	3056	C-H aromatic stretching
3063	3087	3050	3115	C-H aromatic stretching
3500	3459	3138	3434	N-H stretching

<sup>a</sup> Vibrational frequencies calculations are scaled by 0.9614

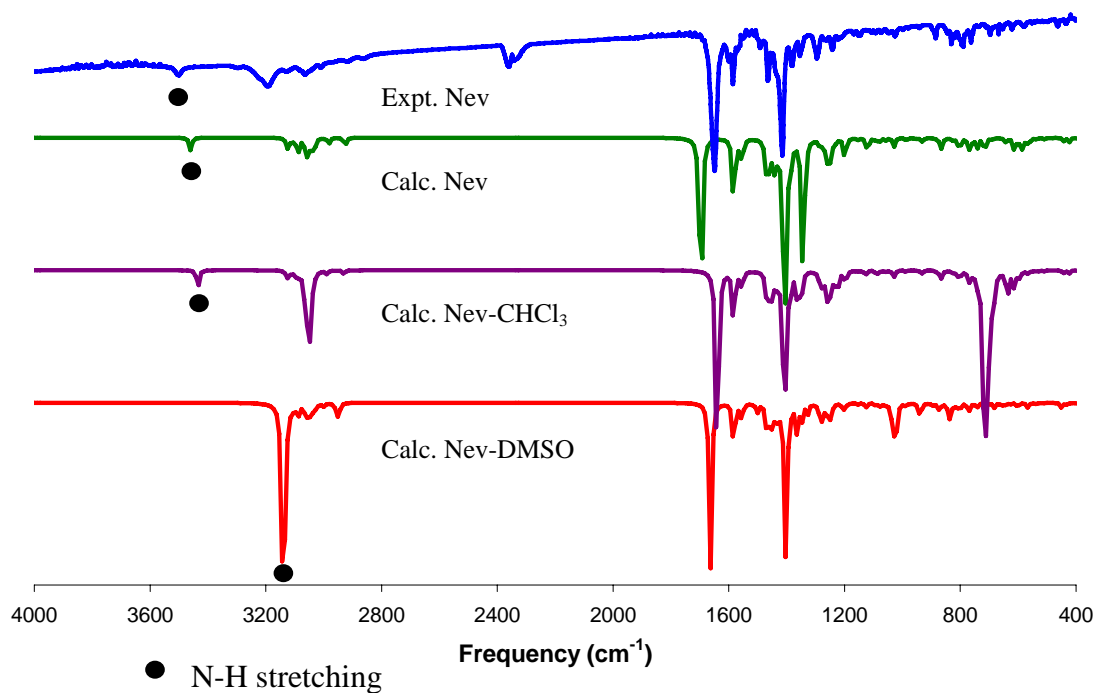


**Figure 19** Comparison of IR spectra of experimental solid nevirapine and calculated of simple nevirapine, nevirapine-DMSO and nevirapine-CHCl<sub>3</sub>

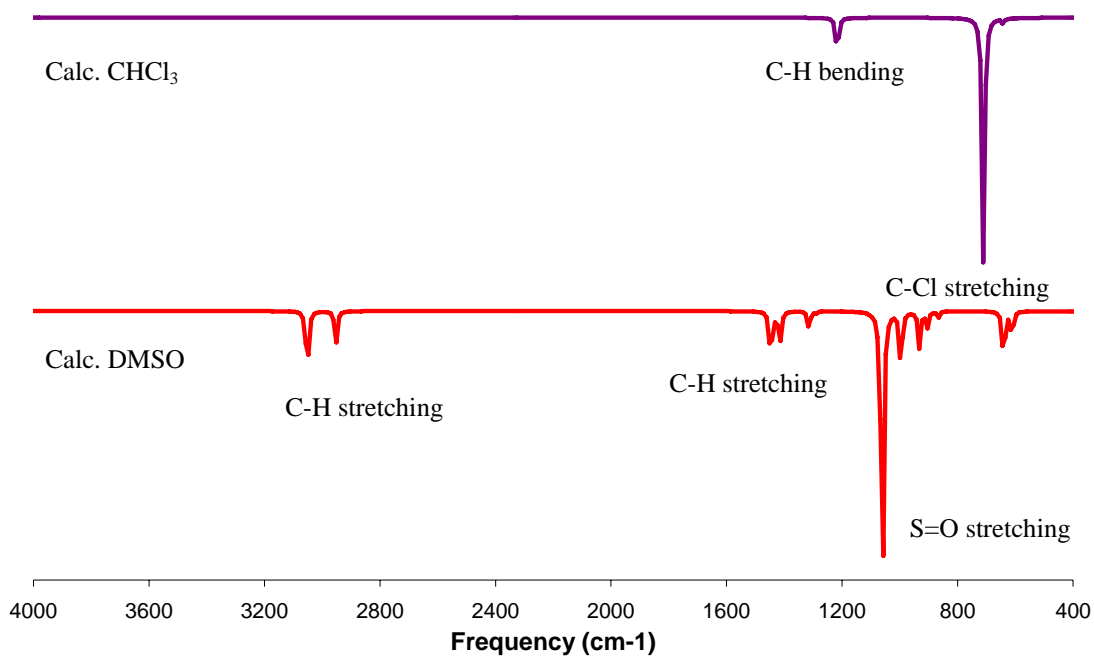


**Figure 20** Calculated IR spectra of DMSO and CHCl<sub>3</sub>

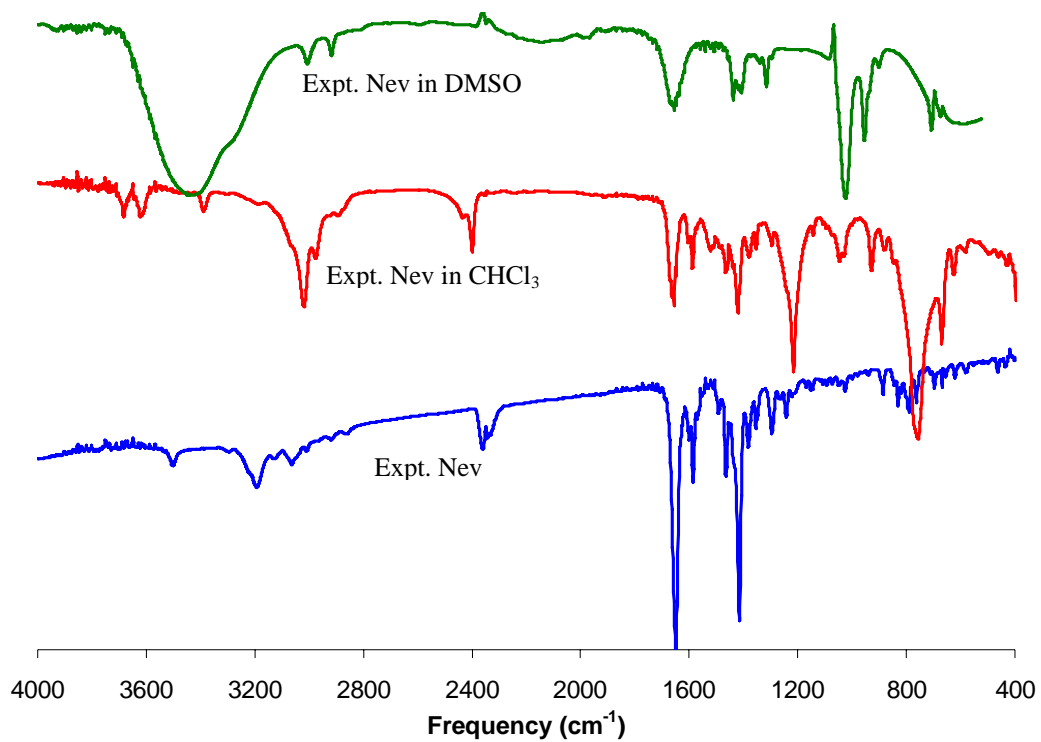


**Figure 21** Experimental IR spectra of nevirapine, nevirapine in DMSO and nevirapine in  $\text{CHCl}_3$